


---

This is the **submitted version** of the article:

Rubio Martínez, Marta; Avci-Camur, Ceren; Thornton, Aaron W.; [et al.]. «New synthetic routes towards MOF production at scale». *Chemical Society Reviews*, Vol. 46, Issue 11 (June 2017), p. 3453-3480. DOI 10.1039/c7cs00109f

---

This version is available at <https://ddd.uab.cat/record/203712>

under the terms of the  <sup>IN</sup> COPYRIGHT license

# New Synthetic Routes towards MOF Production at Scale

Marta Rubio-Martinez,<sup>a</sup> Ceren Avci-Camur,<sup>b</sup> Aaron Thorton,<sup>a</sup> Inhar Imaz,<sup>b</sup> Daniel Maspoch,<sup>b,c</sup> Matthew R. Hill<sup>a,d\*</sup>

<sup>a</sup>CSIRO Private Bag 10, Clayton South VIC 3169 Australia

<sup>b</sup>Institut Català de Nanociència i Nanotecnologia, ICN2, Esfera UAB, Campus UAB 08193 Bellaterra, Spain

<sup>c</sup>Institució Catalana de Recerca i Estudis Avançats (ICREA) 08100 Barcelona, Spain

<sup>d</sup>Department of Chemical Engineering, Monash University, Clayton VIC 3800 Australia. E-mail: [matthew.hill@csiro.au](mailto:matthew.hill@csiro.au)

The potential commercial applications for metal Organic Frameworks (MOFs) are tantalizing. To address the opportunity, many novel approaches for the synthesis of Metal-Organic-Frameworks (MOFs) have been developed recently. These strategies present a critical step towards harnessing the myriad of potential applications of MOFs by enabling larger scale production and hence real-world applications. This review provides an up-to-date survey (212 references) of most the promising novel synthetic routes, i.e. Electrochemical, Microwave, Mechanochemical, Spray drying and Flow Chemistry Synthesis. Additionally, the essential topic of downstream processes, especially for large scale synthesis, is critically reviewed. Lastly we present the current state of MOF commercialization with direct feedback from commercial players.

Marta Rubio-Martínez was born in Barcelona, Catalonia, Spain, in 1982. She received her BSc degree and PhD in Chemistry and her MSc in Nanotechnology at the Universitat Autònoma de Barcelona (UAB) under the supervision of Prof. Daniel Maspoch and Dr. Inhar Imaz. She joined CSIRO Melbourne (Australia) in 2013 as a Postdoctoral fellow. At present, she is a research scientist at CSIRO focusing on extending the capabilities of continuous flow chemistry and material processing, and on scaling-up these processes for large scale production of Metal-Organic Frameworks (MOFs).

Ceren Avci-Camur was born in Ankara (Turkey) in 1989. She received her BSc degree in 2013 and MSc degree in 2015 in Chemistry from Bilkent University (Ankara, Turkey). She is currently pursuing a PhD in Material Science at the Catalan Institute of Nanoscience and Nanotechnology (ICN2) in the Supramolecular Nanochemistry & Materials Group under supervision of Prof. Dr. Daniel Maspoch and Dr. Inhar Imaz in the field of metal-organic nanomaterials with special interest in developing new synthetic pathways for large scale production of metal-organic frameworks in green conditions.

Aaron Thornton completed a Bachelor of Mathematics and Finance at the University of Wollongong Australia in 2005. Since then he has transitioned through a PhD, contributed academically to the field of membranes and adsorbents, and led multiple commercial projects at the CSIRO (Australia's national research agency). He has established a commercial relationship with Air Liquide and multiple academic relationships as a Visiting Scholar through secondment programs with the University of California Berkeley, Chimie ParisTech, Hanyang University, University of Cambridge and the National Technical University of Athens. Dr Thornton has also served as the President of the Membrane Society of Australasia since 2014 and is currently acting as the Product Director for start-up company MOFWORX.

Inhar Imaz was born in Hendaia (Basque Country, France) in 1978. He received his PhD in Materials Science from the Université Bordeaux I in 2005, where he studied the formation of heterometallic metal-organic architectures from tetrahedral building blocks. He joined the CIN-2 (ICN-CSIC) centre in 2005 as a Postdoctoral fellow. At present, he is senior researcher at the Catalan Institute of Nanoscience and Nanotechnology (ICN2). His research interests are focused on controlling the supramolecular assembly of molecules, metal ions and nanoscale building blocks at the macro and nanoscale for the design of novel metal-organic frameworks and functional supramolecular architectures with interesting properties and applications in gas storage, catalysis, etc.

Daniel Maspoch was born in L'Escala (Girona) in 1976. He graduated in chemistry at the Universitat de Girona and obtained his PhD in materials science at the Universitat Autònoma de Barcelona and Institut de Ciència de Materials de Barcelona. After postdoctoral work in Prof. Chad A. Mirkin's group at Northwestern University, he moved to the Centre d'Investigació en Nanociència i Nanotecnologia (ICN-CSIC), thanks to the Ramón y Cajal Program. Since 2011 he is ICREA Research Professor and Group Leader at the Catalan Institute of Nanoscience and Nanotechnology (ICN2). He is interested on controlling the assembly of molecules, metal ions and nanoparticles for the creation of functional nanostructured materials with empty spaces (mainly, MOFs and capsules); and use them in diverse areas, including energy, environment, catalysis and biomedicine.

## **CONTENTS**

### **1. Introduction**

### **2. Production of MOFs: from laboratory to industrial scale**

#### **2.1 Novel Synthesis Routes**

##### **2.1.1 Electrochemical Synthesis**

##### **2.1.2 Microwave Synthesis**

### **2.1.3 Mechanochemical Synthesis**

### **2.1.4 Spray Drying Synthesis**

### **2.1.5 Flow Chemistry**

## **3. Downstream processes**

## **4. Perspectives and commercial developments**

## **5. Conclusions and Future priorities**

### **Acknowledgments**

### **References**

## **1. Introduction**

Metal Organic Frameworks (MOFs) have emerged as a focus of academic fascination and commercial opportunity due to their unprecedented structures that imply a plethora of potential applications. The initial report from Hoskins and Robson instigated a new field of coordination chemistry, combining the tenets of organometallic cluster chemistry with established coordination motifs to form coordination polymers, a.k.a. MOFs.<sup>1,2</sup> Later reports from key instigators including Yaghi,<sup>3,4</sup> Kitagawa,<sup>5,6</sup> Ferey,<sup>7,8</sup> and Long<sup>9,10</sup> projected the potential applications of MOFs, utilising the combination of unprecedented porosity with periodicity and versatile chemistries. The applications envisaged were largely based on separation, storage, sensing or release characteristics.<sup>11-15</sup> As a result, it is possible that MOFs could have revolutionary performance in areas that include natural gas storage,<sup>16-18</sup> petrochemical separation,<sup>19,20</sup> CO<sub>2</sub> capture,<sup>21,22</sup> or drug delivery.<sup>23,24</sup>

However, central to the translation of these new materials into disruptive technologies is the ability to manufacture MOFs at the required scale, purity and price for implementation. For example, the potential application of the enormous natural gas reserves globally as a fuel for vehicles, adsorbed in MOFs within the tank would immediately require megaton scale production of MOFs.<sup>25</sup> Or in CO<sub>2</sub> capture, more than 8000 million tons of CO<sub>2</sub> are produced from coal-fired power stations annually, again requiring many millions of tons of MOF to capture.<sup>26,27</sup> In the laboratory, MOFs are most commonly produced in milligram scales, with multi-day reaction times in expensive organic solvents. Their synthesis is often the balance of a number of competing forces, with a range of kinetic and thermodynamic products possible, meaning that a narrow set of reaction conditions are often possible for a successful synthesis. The large gap between laboratory production and that required for commercial application has created a strong imperative to develop efficient and versatile means of producing MOFs at scale.

As scale up production methods are developed, parameters for assessing their viability have become important. Of these, the key parameter is the space-time yield (STY), a measure of the amount of MOF able to be produced per unit volume of reactor in a 24 hour period. In concert with this, we recently proposed that the absolute value (in g/h) is also important. Many new production techniques are still in the early stages, meaning that the calculated STY may be prone to over-extrapolation. Other important factors are measures of product quality (such as surface area and phase purity), particle size control, yield, and the versatility of the technique. This article will seek to use these criteria in describing the prospective production methods featured herein.

There are several challenges common to the bulk of the prospective scale up methods:

- a) Use of organic solvents. At scale, their cost, toxicity and in some cases flammability become significant issues.
- b) Anion build up. Typically, metal salts are employed as precursor molecules. At scale, nitrates present a safety hazard, and anions such as chlorides can prove corrosive. Oxide and hydroxide metal precursors are preferable.
- c) Ligand availability. Many MOFs require bespoke organic ligands. Production methods that could also produce these starting materials are in development.
- d) Particle size control. Applications such as membranes require nanometre sized particles whereas in storage applications. Larger particles are desired to stop unwanted movement of the MOF particles. Control of this is an important attribute.
- e) Activation. MOFs require removal of non-volatile solvents and unreacted starting materials from their pores. This is a major consideration at large scale.
- f) Shaping of MOF powders produced is also required for using them in real industrial applications.

All these challenges, which are specific for each MOF family due to their different composition and coordination nature, together with their extreme porosity make the synthesis of these materials not as straightforward as for zeolites; meaning that each MOF requires bespoke conditions. In recent years, a number of approaches for addressing these challenges have been considered, including electrochemical, microwave and mechanochemical syntheses as well as spray drying and continuous flow production. Electrochemical synthesis of MOF was developed by BASF and their initial purpose was to exclude anions by using metal electrodes as metal sources. Microwave-assisted synthesis, flow chemistry and spray-drying synthesis allow for a faster crystallization rate and production of smaller MOF crystals. In mechanochemical synthesis, no external heating or solvent is needed, reducing the washing and activation labour after the synthesis.

Given the rapid progress of these techniques, there has been a recent rise in commercial entities that seek to utilise and/or produce MOFs. This review seeks to provide an update on progress of these companies, with direct input from them. BASF pioneered large-scale, bespoke solvothermal techniques primarily for use in vehicular natural gas storage. Following this, spin-out companies have been established, often based upon novel reaction techniques originally developed in a research setting. Some spin-out companies also seek to develop MOF-based products in addition to the broader supply of MOFs to the research community.

In the following, we review the novel synthesis routes developed to date. We also discuss important downstream processing considerations and provide a summary of recent commercial developments.

## **2. Production of MOFs: from laboratory to industrial scale**

In 1995, Nalco Chemical Company and Omar Yaghi claimed the use of solvothermal synthesis to obtain MOFs.<sup>28</sup> Up until now, this synthetic approach is the most common way to obtain grams of MOFs in the laboratory around the world. This method involves mixing solutions of the inorganic salt with the organic linker in a sealed reactor vessel and subsequent heating to promote the growth of insoluble frameworks that precipitate as fine crystals.<sup>29,30</sup> This sealed approach allows the reaction mixture be heated up to temperatures and pressures above the solvent's boiling point to solubilize, partially or completely, otherwise insoluble reagents and form extended networks. It has become a benchmark in MOF chemistry, and a large variety of MOF families such as MIL series,<sup>8,31</sup> MOF-74,<sup>32,33</sup> UiOs<sup>34–36</sup> and PCNs<sup>37,38</sup> have been synthesized following this principle.

However, despite the tremendous academic success that MOFs have had in the last two decades, with thousands of new structures and with very promising applications, only very few of them are produced at large scale and used in real world applications.<sup>18,22,23,39–41</sup> The main reasons for this are the lack of stability of most of the structures towards temperature and humidity, the high cost of the raw materials and, above all, the difficulty of scaling up the synthesis and the post-synthetic stages in a cost-effective way maintaining the product quality and reproducibility between batches. In addition, while the solvothermal approach is a well-known industrial method for chemical synthesis, its application for large scale MOF production is not feasible as MOF synthesis relies on the nucleation at a reactor vessel surface. Up-scaling the reactor vessel significantly decreases the surface to volume ratio and consequently, reduces the efficiency of the reaction. Additional problems include: long reaction times (hours or days), large amounts of solvents used, low quality of materials obtained, high complexity and cost in the up-scaling.<sup>42</sup>

In order for any production MOF process to be industrially viable a number of key aspects have to be considered: (i) a versatile method is crucial in order to accommodate the maximum number of MOF structures with the same piece of equipment; (ii) the possibility to avoid harsh processing conditions such as high temperature and pressure will reduce capital and operating costs and alleviate safety concerns; (iii) a switch from batch to continuous

processing would be beneficial offering higher output per unit time and a continuous steady-state operation leading to significantly reduced downtimes, labour costs, reactor volumes, as well as constant and consistent production; and (iv) a high space-time-yield (STY) parameter which measures the amount of MOF produced per  $\text{m}^3$  of reaction mixture per day.

All these factors make the scale-up of MOF production challenging and have motivated many researchers and engineers to explore and develop novel and commercially viable routes to produce MOFs in an efficient, reproducible and cost-effective way.<sup>43,44</sup> Figure 1 shows the timeline of the most common synthetic processes developed in the last two decades. In this review, we will focus on energy-efficient processes with reduced reaction times that facilitate the up-scaling and the continuous operation. In the following sections, we will describe in detail the advances in electrochemical,<sup>45</sup> microwave<sup>46</sup> and mechanochemistry<sup>47</sup> approaches and the more recent routes, the spray dryer<sup>48</sup> and flow chemistry<sup>49</sup>.

- **Insert Fig 1** -

## **2.1 Novel Synthesis Routes**

### **2.1.1 Electrochemical Synthesis**

Electrochemistry can be defined as the study of interconversion between chemical and electrical energy. It combines electricity and chemistry and deals with chemical changes caused by an electrical current.

Taking advantage of the potential of electrochemistry to synthesize materials and their large experience in the domain, the company BASF first patented the use of electrosynthesis to produce MOFs in 2005.<sup>50</sup> The synthesis consisted on immersing a copper plate in a solution containing the organic linker, 1,3,5-benzentricarboxylic acid (BTC), and an electrolyte. The copper plate, which acts as the electrode, was used as the source of Cu(II) ions. When a certain current or voltage was applied, the Cu(II) ions were released from the copper electrode to the solution and reacted with the dissolved linker. In this patent, a powder of electrochemically produced HKUST-1 that consisted of octahedral crystals (size: 0.5 - 5  $\mu\text{m}$ ) could be fabricated after applying a voltage of 12-19 V and a current of 1.3 A for 150 minutes. The surface area of this synthesized HKUST-1 was  $1820 \text{ m}^2 \cdot \text{g}^{-1}$ , which is higher to that reported for the solvothermally synthesized HKUST-1 ( $1550 \text{ m}^2 \cdot \text{g}^{-1}$ )<sup>51</sup>.

Since this first patent, electrochemical synthesis of MOFs has attracted great attention because it can offer many advantages. One of them is the possibility to run the synthesis of MOFs in a continuous way. It also allows their synthesis under milder conditions than typical solvothermal or microwave syntheses, reducing the reaction time. Indeed, while solvothermal synthesis might take hours or days, electrochemical methods can produce the MOF material within minutes or hours. In addition to these, the electrochemistry method provides the ability to control the MOF synthesis directly during the reaction by controlling the passed current or applied voltage. Finally, the electrochemistry method offers the possibility to synthesize homogeneous thin films or coatings.<sup>52</sup>

Electrosynthesis of MOFs can be classified in two main methods: i) the anodic dissolution, which was the first route patented by BASF; and ii) the cathodic deposition. In the anodic deposition, an applied electric potential induces the release of metal ions from the electrode, which then react with an organic linker present in the solution leading to the formation of a MOF film. In this case, the use of a metallic electrode (instead of metal salts) as the source of metal cations avoids the formation of any corrosive anions (mainly, nitrate and acetate anions) or any by-products. The anodic dissolution is typically carried out in a two-electrode set-up without a reference electrode, and the use of protic solvents is usually needed to ensure the evolution of hydrogen and avoid the reduction of metal ions at the counter electrode. In addition, the use of a sacrificial compound (*e.g.* acrylonitrile, acrylic or maleic esters) that are preferentially reduced or a counter electrode with a suitable overpotential for hydrogen evolution is recommended.<sup>53</sup> In the cathodic deposition, a solution containing the organic linker, the metal ions, and a so-called probase is contacted with a cathodic surface. In this approach, the MOF film deposition results from increasing the pH near the cathodic surface, where the electrochemical reduction of the probase occurs. An example of a probase is the nitrite ions coming from the reduction of nitrates, which are able to deprotonate the organic linker and form the MOF.<sup>54</sup>

**-Insert Table 1-**

Since the electrochemical synthesis of HKUST-1 by BASF using the anodic dissolution was reported, there have been many efforts to understand and optimize this new route (Figure 2a). Fransaer *et al.* recently proposed a mechanism for the anodic dissolution synthesis of HKUST-1 that consists in four phases: (i) initial nucleation; (ii) growth of HKUST-1 islands; (iii) intergrowth; and (iv) crystal detachment.<sup>55</sup> When an electric potential is applied, the oxidation of the anode starts and the Cu(II) ions are released in the solution. The nucleation of the HKUST-1 phase starts once the critical ion concentration on the surface of the anode is reached. The nucleation is progressive and the dimensions of the crystals depend on the synthesis time and choice of the solvent. The HKUST-1 layers grow at the MOF-solution interface confirming that Cu(II) ions, which are dissolved at the interface, diffuse through the HKUST-1 crystals before they react with the organic linker. This migration of ions is accompanied by the creation of voids at the substrate-HKUST-1 interface, resulting in the formation of fragile layers of HKUST-1 crystals that are easily detached from the substrate. Simultaneously, van der Veen and Domke *et al.* described this anodic dissolution mechanism from a more chemical point of view.<sup>56</sup> These authors identified that chemical species involved in the electrosynthesis of HKUST-1 are initially Cu(I)<sub>2</sub>O, which results from the oxidation of the copper plate in the presence of H<sub>2</sub>O or O<sub>2</sub>. Then, Cu(I)<sub>2</sub>O is further oxidized to Cu(II)O that can react with the organic linker and lead to the formation of HKUST-1 crystals.

**-Insert Figure 2-**



To date, it is known that small variations of the applied electric potential and passed current, nature of the solvent and its conductivity, and nature of the electrolyte have a strong influence on the anodic dissolution synthesis of HKUST-1. For example, the applied electric potential is important due to the direct influence on the generation of Cu(II) ions from the copper electrode. As observed by De Vos *et al.*, higher voltages applied by square wave functions provided higher concentration of Cu(II) cations because of the higher dissolution rate of the copper metal (Figure 2b). These conditions let to the formation of coatings with smaller crystals of HKUST-1 in agreement with the nucleation theory.<sup>57</sup> In the same line, Gascón *et al.* observed better results in terms of HKUST-1 coverage of the electrode when square wave functions were used instead of a continuous mode.<sup>58</sup> Denayer *et al.* found that the frequency of these square wave functions does not influence the HKUST-1 coating of the copper electrode.<sup>59</sup>

Solvent media is also influencing the electrochemical crystallization of HKUST-1. De Vos *et al.*<sup>57</sup> and Denayer *et al.*<sup>59</sup> observed the formation of larger crystals when the amount of water (from 10 to 50 % in volume) was increased in the electrolyte water/ethanol solution because it slowed down the reaction by the hydration of the Cu(II) cations. In addition, detachment of HKUST-1 crystals from the electrode was observed for water contents higher than 50 %. Under these conditions, Gascón *et al.* detected the formation of a secondary phase consisting of a catena-triaqua- $\mu$ -(1,3,5-benzene-tricarboxylate)-copper(II) compound.<sup>60</sup> More recently, Deyaner *et al.* investigated the effect of other organic solvents (*e.g.* methanol, ethanol, 2-propanol, acetonitrile, N,N-dimethylformamide (DMF), and dimethylsulfoxide (DMSO)) in the electrochemical formation of HKUST-1 (Figure 2c).<sup>61</sup> They observed that the crystal size increases when increasing the water content in methanol and ethanol; less dense and uniform HKUST-1 layers are obtained in 2-propanol; HKUST-1 crystal morphology is different when using acetonitrile instead of methanol or ethanol; octahedral crystals are generated in DMF; and the amount of water does not influence the synthesis of HKUST-1 in DMSO, as it does in methanol or ethanol.

Because of the low conductivity of the reaction media, electrolytes that enhance charge transport in solution are generally used. Tributylmethylammonium methyl sulfate (MTBS) is usually recommended for syntheses carried out in organic media and, indeed, it showed a positive role on the HKUST-1 synthesis. For example, increase of conductivity by increasing the concentration of MTBS in the electrolyte solution reduced the ohmic drop of the solution and increased the production yield of HKUST-1. However, Deyaner *et al.* found some disadvantages related to the use of MTBS in the electrochemical formation of HKUST-1 thin films. They observed structural damages of the copper mesh and the generation of non-adhesive HKUST-1 crystals to the surface of the anode. On the contrary, they could get more control over the synthesis in the absence of MTBS because of lower current density in the system.<sup>62</sup> Another disadvantage of using MTBS was reported by Hartmann *et al.*, who observed a decrease in the surface area of HKUST-1 that was attributed to the presence of the electrolyte salt in its pores.<sup>63</sup>

Beyond the archetypical HKUST-1, the syntheses of other MOFs have been envisaged using anodic dissolution. Remarkably, Gascón *et al.* demonstrated the possibility to electrochemically synthesize ZIF-8, MIL-53 and MIL-100(Al).<sup>58</sup> Since then, De Vos and Franssaer *et al.* optimized the quality of the synthesized MIL-100(Fe) by performing the electrochemical synthesis under high pressure and high temperature.<sup>64</sup> Also, Attfield and Dryfe *et al.* improved the synthesis of zeolitic imidazolate frameworks (ZIF) (*e.g.* ZIF-4, ZIF-7, ZIF-8, ZIF-14, and ZIF-67) coatings (Figure 2d) by increasing the reaction times (a proxy for higher metal ion concentration), the organic linker concentration and the reaction temperature.<sup>65</sup> With this anodic dissolution, luminescent rare earth based

MOFs were also prepared by Fransaer *et al.* on electrically conductive solid substrates.<sup>66</sup> Here, Tb-BTC and Gd-BTC layers were electrochemically synthesized on terbium and gadolinium metal foils by immersing the foil in a water–ethanol solution containing the organic linker, the electrolyte (MTBS) and applying a constant current of 1 mA/cm<sup>2</sup>.

Within this variety of MOFs, the electrochemical synthesis of MOF-5 has also been largely investigated. Cao *et al.* reported the anodic dissolution electrosynthesis of thin films of rod-like MOF-5 crystals.<sup>67</sup> They could generate dense and thick MOF-5 films by using zinc electrodes in an aqueous solution containing H<sub>2</sub>BDC and ammonium fluoride as the electrolyte salt and applying voltage (2 V) at 65 °C. Liang *et al.* synthesized MOF-5 in the form of flower shape by using molten salt in the electrolyte solution and 1-butyl-3-methylimidazole (BMiM) bromine as a template (Figure 2e).<sup>68,69</sup> This MOF-5 was synthesized using a zinc plate as the anode, a titanium plate as the cathode, and a DMF and BMiM bromide mixture containing H<sub>2</sub>BDC and zinc nitrate hexahydrate as the electrolyte solution. The reaction was done in atmospheric conditions and applying a current density of 0.025 A·cm<sup>-2</sup> for 2 hours.

### -Insert Figure 3-

As state above, the second main route for the electrochemical synthesis of MOFs is the cathodic deposition. In 2011, Dinca *et al.* first investigated the cathodic deposition of MOFs<sup>70</sup> to resolve two major limitations of the anodic dissolution (Figure 3a): i) the deposition surface (anode surface) is used to produce the metal cations and thus, it is eroded in a continuous manner throughout the synthesis; and ii) the selection of the anode metal is limited since the anode is also used as the metal resource. In this cathodic deposition, the metal salt, which is dissolved in the electrolyte solution together with the organic linker and the probase, is used as the metal precursor. To show the potentiality of this approach, Dinca *et al.* showed the synthesis of HKUST-1 and MOF-5 in only 15 min at room temperature (Figure 3b). For it, they used fluorine doped tin oxide (FTO) as the working electrodes, Ag/Ag(cryptand) as the reference electrode, and a DMF:water (100:1) (v:v) mixture containing the organic linkers and the metal salts as the electrolyte solvent. In these syntheses, it was found that the nature of the metal salt plays a crucial role. This importance is due to the nature of the counteranions, which act as a probase, can inhibit or favour the formation of the desired MOF.<sup>71</sup> For example, as the synthesis of MOF-5 starts with the formation of Zn<sub>5</sub>(OH)<sub>8</sub>(H<sub>2</sub>O)<sub>2</sub>(NO<sub>3</sub>)<sub>2</sub>, the use of chlorine anions can inhibit its formation due to the formation of Zn<sub>5</sub>(OH)<sub>8</sub>(Cl)<sub>2</sub>(H<sub>2</sub>O)<sub>2</sub>. On the contrary, the use of nitrate anions can help on its formation since they can act as the probase and participate in the formation of the intermediate specie.

The aptitude of the cathodic deposition to favour the formation films was also exploited by the same authors to form more complex biphasic MOF thin films at room temperature from single deposition baths using potential bias as the main user input.<sup>72</sup> In this case, bilayer structures of MOF-5 and (Et<sub>3</sub>NH)<sub>2</sub>Zn<sub>3</sub>(BDC)<sub>4</sub> (applied potential: -1.7 V) (Figure 3c), mixed structures of MOF-5 and (Et<sub>3</sub>NH)<sub>2</sub>Zn<sub>3</sub>(BDC)<sub>4</sub> (applied potential: -1.1 V), and layers of only (Et<sub>3</sub>NH)<sub>2</sub>Zn<sub>3</sub>(BDC)<sub>4</sub> (applied potential: -1.5 V) were fabricated tuning the applied potential.

Latter innovations on the electrochemical synthesis of MOFs have been centered on the development of new methodologies such as electrophoretic deposition,<sup>73,74</sup> galvanic displacement,<sup>75</sup> anodic-cathodic deposition<sup>76</sup> or bipolar electrochemistry.<sup>77</sup> For example, Ameloot *et al.* combined both anodic and cathodic deposition to perform the modulated synthesis of UiO-66 simultaneously on both anode and cathode surfaces.<sup>76</sup> For this synthesis, zirconium films were used as electrodes and H<sub>2</sub>BDC was dissolved in a mixture of DMF, nitric acid (electrolyte), water and acetic acid (AA). AA was used as a modulator to increase the amount of linker defects and therefore, the BET surface area. However, increase of AA also decreased the crystallinity because of the increase of the competition between BDC and AA. It was found that denser packed films with smoother surfaces were formed on the anode when an AA concentration of 0.5 M or 1 M was used, and that larger octahedral UiO-66 crystals were obtained for AA concentrations higher than 5 M. In this process, when the AA concentration increased, the complexation of released Zr (IV) ions also increased leading to a decrease of the anodic deposition. On the contrary, when the concentration of AA decreased, the concentration of released Zr(IV) ions increased, thereby increasing the deposition on the cathode.

Another interesting example was reported by Bradshaw and Kuhn *et al.* who used bipolar electrochemistry (BE) to produce Janus-type MOF composites inducing the site selective ZIF-8 or HKUST-1 crystallization on a polarized metallic wire under an electric field. In BE, a conducting object is exposed to an electric field established between two electrodes in a solution this induces a positive and negative polarization between the two opposite sides of the object and a redox reactions can occur.<sup>77</sup>

### 2.1.2 Microwave Synthesis

Microwave (MW) irradiation is a widely used method in organic chemistry. In recent years it has been used for the synthesis of inorganic nanomaterials - zeolites and MOFs, among others.<sup>78-81</sup> The method is based on the interaction of electromagnetic waves with any material containing mobile electric charges, such as polar molecules in a solvent or conducting ions in a solid. Contrary to classical solvothermal methods, where thermal energy is transferred from the heat source to the solution through the reaction vessel, in MW synthesis the irradiation interacts directly with the reactants, resulting in more efficient and faster heating. Additionally, in MW synthesis crystallisation occurs at the hot spots that form due to the direct heating of the solvent, in contrast to the wall of the reactor vessel as with conventional heating methods. Consequently, it is much faster and results in a smaller particle size. In this section, we describe some remarkable examples of the preparation of MOFs *via* microwave irradiation.

The pioneering work on MW synthesis of MOFs by Jung *et al.* reported the water-based synthesis of the chromium trimesate MIL-100 MOF in the presence of hydrofluoric acid.<sup>82</sup> The synthesis was performed in a microwave oven at 220 °C for 1, 2 or 4 hours with the reaction mixture in a sealed Teflon autoclave. The results showed the presence of unreacted metallic chromium species for reaction times less than 2 hours. The crystal yield obtained after 4 h was 44 %, which is comparable to the 45 % achieved in the conventional synthesis in 4 days. Two years later, the same group reported the synthesis of spherical nanocrystals of chromium terephthalate

MIL-101 MOF.<sup>83</sup> In this work, they showed that crystal size increases with increasing irradiation time, ultimately allowing the isolation of particles with a high surface area.

The MW synthesis of IRMOF-1, IRMOF-2, and IRMOF-3 was reported by Ni *et al.* who obtained microcrystals with a relatively uniform size and identical cubic morphology in less than 2 minutes.<sup>84</sup> They showed that the crystal size can be varied from micrometer to submicrometer by manipulating the concentration of the starting material. The same synthesis was conducted by Choi *et al.* who investigated how the power level, irradiation time, temperature, solvent concentration and substrate composition affected the crystallinity and morphology of MOF-5.<sup>85</sup> The microwave irradiation lead to crystals after only 30 mins of reaction time while 24 h were necessary with the conventional method. The optimum microwave conditions lead to uniform cubic crystals with average size of 20–25  $\mu\text{m}$  and with a BET surface area of 3008  $\text{m}^2/\text{g}$ .

MW irradiation is an attractive method to synthesize MOFs with biomedical applications, such as iron-carboxylate MOFs, because uniform nanocrystals are easily achievable. For instance, in 2009, Lin and co-workers described the MW synthesis of 200 nm nanoparticles of iron-MIL-101 MOF and its amino functionalized version.<sup>86</sup> The starting materials were dissolved in DMF and then rapidly heated to 150 °C and held at this temperature for 10 minutes.

Several studies have been performed comparing conventional electric (CE) heating, MW and ultrasound (US) methods in order to understand the accelerated US and MW syntheses.<sup>87–90</sup> For example, in 2009, Haque *et al.* performed a kinetic study on the synthesis of MIL-53-Fe.<sup>91</sup> They found that the crystallisation rate (both nucleation and crystal growth) decreased in the order: US>MW>>CE. These results suggested that physical effects, such as hot spots, are more important than chemical effects in the accelerated syntheses performed under US and MW conditions (see Fig.4). A similar study was performed by Chalati *et al.* where the synthesis of iron fumarate MIL-88A nanoparticles was compared with the classical solvothermal, MW and US methods.<sup>92</sup> With the CE heating a polydisperse sample of 200 nm nanoparticles were obtained, whereas 100 nm monodisperse nanoparticles but with very low yields were obtained with the US method and <100 nm monodispersenanoparticle with high yields were obtained with the MW method.

- **Insert Fig 4** -

The zeolitic imidazolate framework, ZIF-8, has been synthesized with MW irradiation and CE heating at 140 °C in 4 hours and 20 hours respectively.<sup>93</sup> In addition to the reduced reaction time, the ZIF-8 obtained by microwave heating had a larger surface area and micropore volume compared with the ZIF-8 synthesized with CE heating.

There are a few reports available showing the effectiveness of MW irradiation for the synthesis of lanthanide–organic frameworks. For example, Silva *et al.* obtained quality single-crystals of the microporous cationic  $[\text{Ce}_2(\text{pydc})_2(\text{Hpydc})(\text{H}_2\text{O})_2]\text{Cl}$  (where pydc corresponds to the 2,5-pyridinedicarboxylic acid) by

applying MW heating for 20 min at 200 °C.<sup>94</sup> In 2014, Vilela *et al.*, synthesized a series of lanthanide (Eu, Gd and Tb) bisphosphonates using conventional hydrothermal synthesis (180 °C, 3 days), MW-assisted heating (40 °C, 5 seconds) and US-assisted synthesis (room temperature, 5 minutes).<sup>95</sup> Under CE heating, microcrystalline materials were obtained which did not possess any significant catalytic activity, whereas the application of MW and US resulted in nanocrystals that exhibited relatively high catalytic activity and excellent selectivity to 2-methoxy-2-phenylethanol (100% yield within 48 hours of reaction time). A recent work by Cao and co-workers showed the gram scale production of a 9 isostructural microporous lanthanide MOFs *via* a microwave over 5 min.<sup>96</sup> The same synthesis but under conventional solvothermal reaction required seven days to produce the same materials with a similar yield. Moreover, with the solvothermal method only 10 milligrams of quality material could be obtained while MW synthesis yielded up to 2 grams.

In recent years, zirconium-based MOFs have attracted great attention due to their exceptionally high thermal and chemical stability. In 2013, D'Alessandro and co-workers reported the efficient synthesis of MIL-140A, MIL-140B and MIL-140A-NH<sub>2</sub> frameworks using MW irradiation.<sup>97</sup> They obtained products with purer phase and higher quality in significantly less time than the CE heating method. Recently, a process optimisation for the UiO-66 MW assisted synthesis was presented by Taddei and co-workers.<sup>98</sup> The optimized synthesis required 15 minutes of pre-mixture of the initial solutions and 15 minutes at 120 °C. The reaction yield was 83% and no significant negative effects on morphology, crystal size, or defects were found from the use of MW assisted heating in comparison with those synthesized by CE heating. One exciting area that it has been explored with MW in the last 2 years is the defect engineering of UiO-66. Babarao and co-workers presented an experimental and theoretical study showing the correlation between the defect concentration composition in UiO-66 and their carbon dioxide adsorption properties.<sup>99</sup> They presented a detailed MW-assisted solvothermal synthesis protocol to prepare pure phases of high-quality crystalline UiO-66 frameworks with different defect concentrations. Highly crystalline UiO-66 octahedral shaped crystals were obtained in a short reaction time of 5 minutes using hydrochloric acid and formic acid as modulators.

### 2.1.3 Mechanochemical Synthesis

Mechanosynthesis is a well-known technique in metallurgy and mineral processing but within the last few decades it expanded rapidly into many areas of chemistry such as catalysis, inorganic chemistry and pharmaceutical synthesis.<sup>100-103</sup> The central concept behind this synthetic method is to promote chemical reactions by milling or grinding solids without any or with only minimal amounts of solvents.<sup>104,105</sup> With this approach the conventional solvothermal MOF reactors are substituted by a mortar and pestle or in a mechanical process by automated ball milling. In general, the mechanical milling process is higher in energy and ensures the reproducibility between batches. In addition to the solvent-free conditions, this approach leads to a faster and more efficient synthesis of MOFs obtaining quantitative yields and allows to use MOF precursors with low solubility such as oxides, hydroxides and carbonates. However, the big limitation lies in up-scaling mechanochemical synthesis, it is essentially a batch processing technique with a relatively low rate of production. Furthermore, it should be noted that despite a 'solvent-free' synthesis, purification may still be needed and may require a solvent.<sup>106</sup> Nevertheless this synthetic

approach is the most environmentally friendly process to produce MOFs, and hence could reduce significantly the cost of production.<sup>107,108</sup>

The three different mechanochemical approaches used for MOF production are Solvent-Free Grinding (SFG) which is the simplest method and avoids the use of solvent; Liquid-Assisted Grinding (LAG) which is more versatile, and quicker, as it uses catalytic amounts of liquid phases which increase the mobility of the reagents; and finally, Ion-and-Liquid Assisted Grinding (ILAG) which uses a catalytic liquid with traces of salt additives to accelerate the MOF formation. Using these techniques, the synthesis for almost all families of MOFs has been demonstrated, and selected studies will be explained in this section.<sup>109</sup>

A first work by James and co-workers employed the SFG method, milling a dry mixture of copper acetate and isonicotinic acid (Hina) powder for 10 minutes resulting in the formation of copper(II) isonicotinate MOF with acetic acid and water molecules occluded in the pores (see Fig 5a).<sup>110</sup> Using the same approach, the same group performed a screening study, grinding sixty different combinations of twelve different divalent metal salts, composed of copper, nickel and zinc together with five 5 different carboxylate organic linkers for 15 minutes.<sup>111</sup> As a result several crystalline structures, including two microporous metal-organic frameworks HKUST-1 and Cu(INA)<sub>2</sub> were obtained.

One important advantage of this approach is the possibility to synthesize MOFs with only water as a by-product allowing the complete elimination of the purification stage. This is achieved by using hydroxides or oxides as a metal source which then in combination with the protons generated from the organic ligand forms H<sub>2</sub>O.

Following this strategy, Tanaka and co-workers presented the mechanical dry conversion of zinc oxide and an imidazole ligand into ZIF-8.<sup>112</sup> The process was investigated for reaction times of 3 to 240 hours, yielding the best BET surface area (1480 m<sup>2</sup>/g) at 96 hours. The decrease of the BET surface area after 96 hours was due to the formation of amorphous domains during the mechanochemical reaction. The same year, Balema and co-workers reported the preparation of the yttrium based MIL-78 MOF under completely liquid-free conditions and using a metal hydride for the first time as a starting material and forming hydrogen as a by-product.<sup>113</sup>

Very recently, Xu and co-workers reported the synthesis of MIL-101 (Cr) without the addition of solvent and hydrofluoric acid.<sup>114</sup> The chromium salt and the terephthalic acid were ground for 30 minutes at room temperature and then transferred into an autoclave at 220 °C for 4 hours, yielding a material with a BET surface area of 3517 m<sup>2</sup>/g and with a reduced particle size compared to the batch process.

- **Insert Fig 5** -

In 2006, Braga and co-workers demonstrated for the first time how the addition of small amount of solvent to the powder mixture precursors could effectively improve the crystallisation of the compounds and accelerate the

synthesis.<sup>115</sup> They synthesized the  $\text{CuCl}_2(\text{dace})$  (where dace is the trans-1,4-diaminocyclohexane) one-dimensional coordination polymer by grinding the starting materials for 5-10 minutes in the presence of water or DMSO which were then removed by thermal and vacuum treatment. In 2009, Frišćić and Fábíán demonstrated the ability to selectively and quantitatively build different metal-organic architectures by simply changing the amount and type of solvent using the same starting materials. In this specific work, they presented the formation of four coordination polymers and two porous structures by grinding zinc oxide and fumaric acid in the presence of different types of solvents.<sup>116</sup> In 2010, Klimakow *et al.* synthesized the well-known HKUST-1 and its benzenetribenzoate-based analogue MOF-14 *via* the LAG approach. The MOFs were obtained by grinding the copper acetate monohydrate salt with the corresponding organic linkers for 25 minutes. As a by-product, acetic acid was formed, which blocked the micropores and consequently resulted in a smaller BET surface area compared to other synthetic approaches.<sup>117</sup> James and co-workers showed that by adding small amounts of liquid by-products, generated *via* the SFG method, before the mechanical process, that the synthesis could be accelerated.<sup>118</sup> By adding small amounts of acetic acid into the precursor mixtures, the formation of  $\text{Cu}(\text{INA})_2$  MOF was dramatically accelerated, while for HKUST-1, due to the lower solubility of the trimesic acid, no improvement was reported. In 2010, the same group studied by X-ray diffraction the structural properties of  $[\text{Zn}_2(\text{fma})_2(\text{bipy})]$ , where fma corresponds to fumaric acid and bipy to 4,4'-bipyridine, prepared by mechanochemical synthesis (see Fig.5b).<sup>119</sup> The acetic acid and  $\text{H}_2\text{O}$  by-products occluded in the pores were removed by thermal treatment and the interpenetrated structure was refined using Rietveld methods.

In 2015, Prochowicz *et al.* described the “SMART” (SBU-based Mechanochemical Approach for pRecursor Transformation) strategy for the synthesis of IRMOFs.<sup>120</sup> The successful mechanochemical synthesis was performed by mixing pre-assembled oxo-zinc amidate clusters with terephthalic acid in the presence of microlitres of N,N-diethylformamide (DEF) over 60 minutes. Additionally, the study showed the importance of the acid-base relationship between reagents in this type of approach.

Recent work by Frišćić and co-workers presented the synthesis of UiO-66 and UiO-66-NH<sub>2</sub> at gram scale by adding different amounts of N,N-dimethylformamide (DMF) and methanol to the solid mixtures of the reactants as well as exposing the powder mixture to methanol vapours at 45 °C for 3 days and 1 week respectively.<sup>121</sup> The best BET surface area obtained for UiO-66 was 1020 m<sup>2</sup>/g with 75 minutes grinding, and 945 m<sup>2</sup>/g for UiO-66-NH<sub>2</sub> after 90 minutes grinding, both in the presence of methanol, for the materials exposed to methanol vapours.

The third mechanochemical methodology, ILAG, was demonstrated to be highly efficient for the synthesis of pillared-layered MOFs. For example, the zinc pillared material based on terephthalic acid and dabco (1,4-diazabicyclooctane) was synthesised after 45 minutes reaction by adding catalytic amounts of an alkali metal or ammonium nitrate salt into the mixture (Fig. 5c).<sup>122</sup> Using the same starting materials, but replacing the ammonium nitrate with sulphates, yielded the same pillared-layered structure but on a hexagonal grid. A second example was presented, showing the mechanochemical ILAG approach for the room-temperature synthesis of ZIF-8, using zinc oxide as the starting material and stoichiometric amounts of ammonium salts.<sup>123</sup> In this case the

use of salts enabled synthesis with imidazole enabling the selective ZIF topology formation by changing the type of ammonium salt and adjusting the reaction times.

Mechanochemistry is a versatile method that allows the synthesis of most of the common MOF structures, however so far all examples described a production at less than one gram scale. As an alternative, extrusion techniques have been explored for the scaling of MOFs under solvent-free conditions. Extrusion is one of the major continuous manufacturing processes used in industries such as food, metallurgy, plastics and pharmaceuticals and has shown very promising results for the synthesis and shaping of MOFs. In 2015, James and co-workers showed the synthesis of HKUST-1, ZIF-8 and aluminium fumarate MOF with twin-screw extrusion (TSE) at the gram scale. Figure 5d shows the TSE used for the synthesis of MOFs which consists of a feed port where the MOF precursors were introduced into a heatable barrel containing the screw and an exit port which a die can be attached to shape the final material. HKUST-1 was synthesized by extruding copper hydroxide and trimesic acid in the presence of methanol. The extrudate was stirred in ethanol and dried at 150 °C for 2 hours yielding a N<sub>2</sub> BET surface area of 1738 m<sup>2</sup>g<sup>-1</sup>. In the case of ZIF-8 the synthesis was performed by a single screw extrusion (SSE) where the zinc carbonate and the 2-methylimidazole ligand were extruded at 200 °C without the addition of any solvent. In this case, the activation was carried out by stirring the material in methanol and drying the material at 150 °C yielding a N<sub>2</sub> BET surface area of 1738 m<sup>2</sup>g<sup>-1</sup>. A last example was obtained by introducing a mixture of aluminium sulphate, sodium hydroxide and fumaric acid into the twin extruder at 150 °C. In this case the by-product was removed by washing the extrudates with water and N<sub>2</sub> BET surface area obtained was 1010 m<sup>2</sup>g<sup>-1</sup>. Extrusion is an efficient way to produce MOFs solvent free with high with very promising space-time-yield (STY) (see figure 5e). Kilogram scale production could be achieved by using a large-scale equipment and paired with a more detailed knowledge and understanding of the MOF synthesis by this methodology.

#### 2.1.4 Spray-Drying Synthesis

Spray-drying (SD) process has been a well-established method in industry for decades. The basic idea behind this method is the production of dispersed powder from a liquid or slurry that is rapidly evaporated with a hot gas. The development of the SD method evolved over a period from 1870s through early 1900s. SD was first patented in 1872 by Samuel Percy,<sup>124</sup> but it was not until the World War II when it gained importance due to transportation needs. SD was used to reduce the weight of food and other species by removing their liquid content (mainly, water). Since then, SD has been widely used for the production of dried pharmaceuticals, bone and tooth amalgams, beverages, flavors, milk and egg products, soaps and detergents, and many other products.<sup>125</sup> More recently in history, SD has extended its use to the encapsulation and miniaturization of multiple species,<sup>126,127,128</sup> with the idea of protecting them, controlling their release, and increasing their solubility and dispersability. It has also been employed for preparing very homogeneous mixtures of reactants,<sup>129,130</sup> a crucial step that has facilitated the fabrication of certain materials.

Beyond the use of SD in these applications, the local heating of micro- and submicrometer droplets that occurs during the SD process can also be used to conduct chemical reactions. Thus far, this concept has mainly been



utilized for discovering and isolating metastable phases of materials that can be only reached thanks to the fast drying conditions of the SD method.<sup>131</sup>

In 2013, MasPOCH *et al.* expanded this concept to the synthesis of supramolecular materials and, in particular, MOFs.<sup>132</sup> The main principle of the process was based on the fast drying of atomized microdroplets of a solution that contains the MOF precursors. (Figure 6a, b) Thus, the process starts with atomization of a solution of the MOF precursors into a spray of microdroplets. This step is accomplished by simultaneously injecting one or more solutions, at a certain rate, (hereafter, *feed rate*) and compressed air or nitrogen gas, at another certain rate (hereafter, *flow rate*). Thus, each precursor droplet contacts -and is suspended by- a gas stream heated to a certain temperature (hereafter, *inlet temperature*), causing the solvent to be heated and evaporated and inducing the MOF precursors (*e.g.* metal ions and organic ligands) to react forming MOF nanoparticles inside each droplet. At this moment, the newly formed MOF nanoparticles accumulate and merge into compact or hollow spherical MOF superstructures/beads while the solvent is fully evaporated. These MOF superstructures/beads are finally collected inside a collector located at the end of the spray drier instrument.

**- Insert Figure 6-**

Table 1 lists all MOFs –together with the optimized conditions and yields- that have been synthesized using the SD method so far. Besides the optimization of the synthetic parameters such as type of reagents/solvents, feed/flow rates and inlet temperature, a very important aspect that needs to be carefully selected when one wants to synthesize a specific MOF by SD is how the precursor solution is introduced into the spray drier. To date, there are four major modes for introducing the MOF precursor solution: i) use of a two-fluid nozzle (Figure 6c); ii) use of a three-fluid nozzle (Figure 6d); iii) use a T-junction (Figure 6e); and iv) use a continuous flow coupled to a reactor (Figure 6f).

**- Insert Table 2-**

The use of two-fluid nozzle is the simplest process. It is based on the preparation of a homogeneous solution or suspension that contains all MOF precursors, which is then injected through a two-fluid nozzle.<sup>132</sup> This two-fluid nozzle allows the simultaneous injection of this precursor solution at a certain feed rate and compressed air or nitrogen gas at another certain flow rate. In general, this method is very useful to synthesize MOFs that are built up from mononuclear metal ions or smaller metal clusters or secondary building-units (SBUs). An archetypical class of MOFs that can be fabricated using this approach is the large family of MOFs constructed from Cu(II) paddlewheel units and polycarboxylate linkers. For example, HKUST-1 (also known as Cu-BTC or Basolite™ C300) can be synthesized by spray-drying a solution of  $\text{Cu}(\text{NO}_3)_2 \cdot 2.5\text{H}_2\text{O}$  and trimesic acid ( $\text{H}_3\text{BTC}$ ) (3:2 molar ratio) in DMF, ethanol and water (1:1:1) with a feed rate of  $4.5 \text{ ml} \cdot \text{min}^{-1}$ , a flow rate of  $336 \text{ ml} \cdot \text{min}^{-1}$  and an inlet temperature of  $180 \text{ }^\circ\text{C}$ . They could be obtained as hollow spherical MOF superstructures (size:  $2.4 \pm 0.4 \text{ } \mu\text{m}$ ) or nanoparticles (size:  $75 \pm 28 \text{ nm}$ ) (Figure 7a).

- Insert Figure 7-

Second and third routes for introducing the MOF precursors inside the spray drier instrument are very similar.<sup>132</sup> They are based on using multi-fluid nozzles, to independently atomize the solutions containing the MOF precursors, or additional channels, to independently inject them. Both approaches enable mixing of the precursor solutions just before they are heated into the atomized droplets. In the first approach, mixing occurs inside the drying chamber, thanks to the coalescence of the atomized droplets, whereas in the second one, mixing is done through a connector inserted before the two-fluid nozzle. Using either variation decreases the probability that unwanted species or micrometre-sized MOFs will form in the precursor solution before it is spray-dried. They also enable use of reagents (*e.g.* bases) to accelerate MOF formation, thus increasing yields and purities and enabling the synthesis of new hollow MOF superstructures and related nanocrystals. To date, both approaches have allowed the synthesis of several MOFs, including MIL-88A<sup>132</sup>, ZIF-8<sup>132,133</sup> and Fe-BTC/MIL-100<sup>133</sup> (Figure 7b,c).

In the last approach, the MOF precursor solution is passed through a continuous-flow reactor just before the entrance of the spray dryer.<sup>134</sup> This process begins by injecting the precursor solution into a continuous coil flow reactor encased in a thermostatic oil tank, where it is heated at a certain temperature ( $T_1$ ) to promote the SBU formation and nucleation. Here, the residence time of the precursor solution in the coil flow reactor is controlled by the rate of the pump (the *feed rate*). Since the outlet flow of the reactor is connected directly to the nozzle of the spray-dryer, the pre-heated solution is automatically injected into the spray-drier at the same feed rate. The solution is then atomised using a two-fluid nozzle, and is dried at a certain inlet temperature and flow rate, such that the MOF growth is confined to the atomised microdroplets.

In most of the cases, this last continuous process enables the collection of dried MOFs shaped in the form of compact micrometre superstructures/beads instead of the hollow ones usually obtained in the first three strategies. This difference is attributed to the formation, inside the reactor, of a suspension containing a primary nucleus. In a general spray-drying process, the atomised droplets are exposed to hot air, the solvent evaporates and consequently, the droplet surface shrinks. During this process, hollow superstructures are formed when there is a non-linear change in precursor concentration at the droplet: specifically, it causes the formation of an impermeable shell and the generation of gas at the core. However, in this latter case, uniform precursor concentration and droplet temperature are reached, owing to the presence of the uniformly-distributed nuclei in the droplet. The rate at which the nucleus can be brought to the surface by diffusion is lower than the rate at which the nucleus can grow during the drying-evaporation process. This difference favours a linear change in precursor concentration and temperature at the droplet, and consequently, drives the formation of dense superstructures.

The main advantage of this last SD approach is that it allows the synthesis of MOFs assembled from high-nuclearity SBUs. Indeed, numerous members of the family of UiO-66 (*e.g.* UiO-66-NH<sub>2</sub>, UiO-66-Br, etc.) as well as Fe-BTC/MIL-100 and [Ni<sub>8</sub>(OH)<sub>4</sub>(H<sub>2</sub>O)<sub>2</sub>(L)<sub>6</sub>]<sub>n</sub> (where L = 1H-pyrazole-4-carboxylic acid) series were synthesized using the resulting spray-drying continuous flow-assisted synthesis. For example, UiO-66 was

synthesized using  $ZrCl_4$  and BDC as reagents, DMF and  $H_2O$  as solvents, an initial concentration of 0.1 M for both reagents, a final molar ratio (Zr/BDC/ $H_2O$ /DMF) of 1:1:30:135, a  $T_1$  of 115 °C; an inlet temperature of 180 °C, and a flow rate of 336  $ml \cdot min^{-1}$ . Under these optimized conditions, in which the amount of water, the feed rate and the coil temperature were found to be very important, UiO-66 was fabricated with a space-time yield of 19.6  $kg \cdot m^{-3} \cdot d^{-1}$  (Figure 7d).

Lastly, the innovations of using SD in the MOF field have been centered on the use of new chemistries to build and/or modify MOFs;<sup>135,136</sup> the synthesis of multivariate or multimetallic MOFs;<sup>137,132</sup> and the mixture of MOFs with other materials to make composites.<sup>132,138</sup> With this aim, the use of SD has been extended to the synthesis of porous materials that are not based on coordination bonds but on hydrogen bonds.<sup>136</sup> For instance, MPM-1-TIFSIX, a porous material based on the hydrogen-bonded assembly of  $[Cu_2(ade)_4(TiF_6)_2]$  (ade = adenine) paddlewheels (Figure 8a), was synthesized by spray-drying an aqueous solution of  $Cu(NO_3)_2 \cdot 2.5(H_2O)$  and  $TiF_6(NH_4)_2$  along with a solution of adenine in water/acetonitrile mixture using a 2-fluid nozzle and an inlet temperature of 150 °C. Moreover, SD was also very recently found to be a fast method to post-synthetically modify MOFs using conventional covalent chemistry (Figure 8b).<sup>135</sup> To perform this modification, a suspension of pre-synthesized MOF crystals are spray-dried together with the desired reagent. With this simple method, two MOFs, the amine-terminated UiO-66-NH<sub>2</sub> and the aldehyde-terminated ZIF-90, were rapidly post-synthetically modified with aldehydes and amines, respectively, using the well-known Schiff-base condensation reaction and achieving conversion efficiencies up to 20 % and 42 %, respectively. Moreover, it was demonstrated that the aldehyde groups of ZIF-90 could be cross-linked using a diamine molecule with a conversion efficiency of 70 %.

#### - Insert Figure 8-

Another advantage of SD as a synthetic method in the MOF field is the possibility to synthesize multi-metallic and multi-variate MOFs. From an experimental point of view, the synthesis of these multi-component MOFs does not require technological changes. Its main principle is based on mixing different metal ions or organic linkers in the MOF precursor solution that is spray-dried. With this approach, Wang *et al.* showed the synthesis of lanthanide-based MOF nanoparticles in which the ratio of Tb(III)/Eu(III) was controlled (Figure 8c).<sup>137</sup> They proved that the resulting MOF nanoparticles could be used as promising nanothermometers with high detection sensibilities, spatial resolutions and short acquisition times. Similarly, multi-variate UiO-66s were synthesized by mixing different ratios of two (benzenedicarboxylic acid and 2-bromobenzenedicarboxylic acid) or three (benzenedicarboxylic acid, 2-aminobenzenedicarboxylic acid and 2-Bromobenzenedicarboxylic acid) organic linkers in the MOF precursor solution (Figure 8d).<sup>134</sup> The resulting UiO-66 materials showed tunable pore surface area. For example, the surface area decreased with increasing equivalents of 2-bromobenzenedicarboxylic acid : 818  $m^2 \cdot g^{-1}$  for 0.6; 678  $m^2 \cdot g^{-1}$  for 1.3; and 570  $m^2 \cdot g^{-1}$  for 2.3.

Finally, SD is also a very simple and fast method to produce MOF-based composites. As above, these MOF-based composites can be created just mixing other materials – pre-synthesized or their precursors for *in-situ* synthesis-

in the MOF precursor solution. With this basic idea, Maspoch *et al.* demonstrated that different substances such as magnetic inorganic nanoparticles (Figure 8e),<sup>132</sup> inorganic salts (NaCl, CaCl<sub>2</sub> and LiCl)<sup>132,139</sup> (Figure 8f) and fluorescent molecules<sup>132</sup> can be combined with MOFs, thereby creating different type of composite materials that combine the intrinsic properties of MOFs and these other materials. Finally, same authors showed that SD method can be also used to combine MOF with organic polymers.<sup>138</sup> In this specific case, pre-synthesized HKUST-1 nanocrystals were encapsulated into polystyrene spheres to improve the hydrolytic stability of HKUST-1.

### 2.1.5 Flow Chemistry

Flow chemistry is a continuous processing technology used in the pharma and agrochemical sectors over the last two decades. Recently, its application to the synthesis of functional nanomaterials such as inorganic nanoparticles, quantum dots, metal oxides and MOFs has shown great promise. Contrary to batch reactions, in a flow chemistry setup, the chemical reactions occur in a continuously flowing stream in a tube or pipe rather than in a reactor vessel. This results in several main advantages: (a) the surface area-to-volume ratio for a reaction mixture in a flow reactor is much higher than in a batch-type reactor giving inherent improvements to heat and mass transfer leading to a much rapid syntheses; (b) flow chemistry allows for precise control over the reaction parameters which facilitates the synthesis optimization and the reproducibility between batches; (c) harsh reaction conditions can be safely reached due to excellent transport intensification properties of the reactors; (d) typically less solvent is used and the energy consumption is lower; (e) downstream processes and quality control methods can be easily integrated in the flow processes and (f) these type of reactors are readily scaled-up. Flow chemistry is thus a cost-effective method that follows the green principle and satisfies the requirements for industrial production. Not surprisingly, several researchers have started to use flow chemistry to synthesize MOFs. In the last year, numerous works have been reported in the literature and in this review we will classify such reports into three different categories : (a) microfluidic reactors (MR), which manipulate the reagents in channels that are geometrically constrained at the microscale; (b) plug flow reactors (PFR) where the reagents are pumped through a tube or pipe and consumed as they flow down the length of the reactor and (c) stirred tank reactors (CSTR) where the MOF precursor are introduced into a tank reactor while products are continuously removed. Table 4 lists all MOFs – together with the optimized conditions and space-time-yields- that have been synthesized using the flow chemistry method so far.

- **Insert Table 3** -

In 2011, Ameloot and co-workers were first to show that microfluidics could be used for the synthesis of metal-organic materials.<sup>140</sup> They synthesized metal-organic crystals in a micro-scale reactor, in which the reagent phases were injected into an immiscible carrier fluid, causing the spontaneous formation of droplets where the reaction occurs (Figure 9b). In this case, the immiscibility of the water and oil phases was exploited as a template for the controlled formation of hollow metal-organic copper trimesate HKUST-1 microcapsules. The authors described the crystallisation process as a dynamic on-going process of nucleation and crystal growth that resulted in the formation of crystalline MOF membranes with a uniform wall thickness.

Two years later, Faustini *et al.* reported the solvothermal and hydrothermal synthesis of MOFs and MOF-composite superstructures using oil microdroplets as a reactors.<sup>141</sup> Four representative MOF structures, copper trimesate HKUST-1, zinc terephthalate MOF-5, zinc aminoterephthalate IRMOF-3 and zirconium terephthalate UiO-66, were synthesised, yielding substantially faster kinetics in comparison to the conventional batch processes (see Fig 9a). In addition, they reported the possibility to create MOF heterostructures using imidazolate frameworks (ZIFs) in a two-step process. Firstly, the iron oxide precursor solution and the oil phase were injected and reacted in a microreactor at 80 °C for 2 minutes. Then, the resulting iron oxide particles were transported downstream to a second microreactor, where they merged and reacted with a mixture of ZIF-8 precursor (zinc nitrate and 2-methylimidazolate in methanol, and polystyrenesulphonate). This lead to the creation of core-shell Fe<sub>3</sub>O<sub>4</sub>@ZIF-8 composite superstructures.

The same year, Coronas and co-workers demonstrated the feasibility of the droplet-based microfluidic approach for the crystallisation of the iron fumarate MIL-88B MOF. In this study, they confirmed that the size of the resulting crystals was dependent of the temperature and residence time. They observed a continuous increase in particle size from average sizes ranging from 90 to 900 nm with higher residence times and/or higher temperatures.

- **Insert Fig 9** -

In addition, D'Arras and co-workers demonstrated the possibility to synthesise new structures using microsystems.<sup>142</sup> They reported the structure of a new cerium(III)-terephthalate MOF which was synthesized in a very short residence time and using a high temperature and pressure flow-type reactor.

The latest MR studies were reported by Polyzoidis *et al.* and Tai *et al.*, where they synthesized ZIF-8 and UiO-66 nanoparticles respectively in a PFA microreactor showing that varying the residence time and the molar ratio of the reaction. They were able to modify the size and shape of the final crystals from a few nanometres to several micrometres.<sup>143,144</sup> As these two last examples showed, microfluidic systems are ideal for reaction optimisation and screening experiments within a laboratory. However, in order to synthesise large quantities of MOFs, it is better to use reactors with larger channel dimensions, as these are more suitable for large volumetric throughput.

Moving to the PFR reactors the first work was reported in 2012 by Gimeno-Fabre *et al.* showed the synthesis of HKUST-1 and Ni-CPO-27 in a counter current mixing reactor where the MOF precursors were mixed with a preheated supercritical water stream at high pressures.<sup>145</sup> The high temperatures were used in order to increase the rate of crystal growth, with a limitation in that heating beyond 300 °C could lead to the formation of metal oxides as a waste-product. Three years later, the same reactor was used to demonstrate the large scale production of ZIF-8 and the control of the size and shape of the crystals by adding ammonium hydroxide or trimethylamine in the reaction mixture.<sup>146</sup> The STY obtained in this process was 11625 kg m<sup>-3</sup>day<sup>-1</sup> and with a surface area of 1800 m<sup>2</sup>g<sup>-1</sup>. Retaining the use of supercritical water and an ethanol stream, Bayliss *et al.* developed a system to produce MIL-53(Al) and HKUST-1 under continuous flow conditions obtaining a STY of 1300 kg m<sup>-3</sup>day<sup>-1</sup> and 730 kg m<sup>-3</sup>day<sup>-1</sup>.

$^3\text{day}^{-1}$ , respectively.<sup>147</sup> These last two methods produced high quality materials with high STY, however high temperatures and pressures were still required, which increase the overall cost of the process and could limit the practicality of the technique at industrial scale.

In 2013 Chang *et al.* reported a proof of concept mesoscale flow production of HKUST-1 using 5 minutes as a residence time and with a surface area of  $1673\text{ m}^2\text{g}^{-1}$ .<sup>148</sup> The particle size of the MOF can be adjusted by changing the relative ratios of the solvents and reaction temperatures from 150 nm to  $4\mu\text{m}$ . To demonstrate the versatility and efficacy of flow reactors to produce MOFs, Rubio-Martinez and co-workers used a PFA reactor to synthesize the copper trimesate HKUST-1, the zirconium terephthalate UiO-66 and the scandium biphenyl-tetracarboxylate NOTT-400, all with different reaction requirements (see Fig. 98).<sup>149</sup> The materials were obtained in 5, 10 and 15 minutes, respectively, without loss in yield or product quality. It was demonstrated that the results could be extended 30-fold in scale, allowing a production rate greater than a kilogram per day and a STY of  $4533\text{ kg m}^{-3}\text{day}^{-1}$  using a bench-top reactor. The successful up-scaling of this process was demonstrated in a second publication where the production of the aluminium fumarate MOF was proved in 4 different stainless-steel tubular flow reactors: a 10 mL coil tubing at laboratory scale, two intermediate stages with 107 mL and 374 mL reactor volume, and a pilot-scale 1.394 L reactor, delivering unprecedented production rates and STYs ( $97\,159\text{ kg m}^{-3}\text{day}^{-1}$ ) while maintaining the product quality.<sup>150</sup> To our best knowledge, this is the highest reported value of STY for a MOF produced by continuous methods. Additionally, the reactor design used in this work demonstrated the possibility to readily translate reaction parameters from the laboratory scale to pilot scale without any re-optimization of the reaction conditions, while maintaining the STY values within the same range.

The last work using PFR comes from Stock and co-workers who presented the synthesis of UiO-66, CAU-13 and STA-12 - a new cadmium phosphonate network using a 16 mL PTFE reactor yielding a STY of  $428\text{ kg m}^{-3}\text{d}^{-1}$  and  $3049\text{ kg m}^{-3}$  for UiO-66 and CAU-13, respectively.<sup>151</sup> One year later, the same was group reported the water-based synthesis the zirconium fumarate and UiO-66-NH<sub>2</sub> starting from a slurry of the starting solutions.

In a slightly different reactor design, two recent works reported the combination of microwave assisted heating with PFR system. The first study from 2015 by Albuquerque *et al.* reported on a system where the microwave reactor was attached to the flow reactor in order to accelerate the nucleation of the MOFs and to improve the reproducibility of the synthesis.<sup>152</sup> The MOF precursors of MOF-74(Ni) were introduced first into the nucleation zone that consisted of a microwave reactor and consequently the material was introduced into a PFA coil for 8 min to growth the final crystals. As a result, they obtained a better crystallinity in a shorter reaction time and achieved a STY of  $2160\text{ kg m}^{-3}\text{day}^{-1}$ . The second work by Taddei *et al.* presented the synthesis of UiO-66, HKUST-1 and MIL-53(Al) in a 6.2 and 53 mL PTFE flow reactors heated by microwave.<sup>153</sup> The materials were obtained in 7, 1 and 4 minutes of residence time, while maintaining the product quality and resulting in high STY of  $7204\text{ kg m}^{-3}\text{d}^{-1}$ ,  $64800\text{ kg m}^{-3}\text{day}^{-1}$  and  $3618\text{ kg m}^{-3}\text{day}^{-1}$  for UiO-66, HKUST-1 and MIL-53(Al) respectively.

The use of stirred CSTR was showcased by two groups, synthesizing NH<sub>2</sub>-UiO-66 and MOF-5. The first work in 2013 by Schoenecker and co-workers who synthesized the amine-functionalised UiO-66 in DMF by convention heating.<sup>154</sup> In this system the MOF precursors were pumped into a pre-mixing tank over 15 min and then introduced into a 2 litre flow crystallisation reactor over 8 to 40 hours during which time small aliquots of the intermediate product were collected at different times to bulk reaction kinetics. The product obtained had good crystallinity but the BET surface area and the yield were below the values reported in batch. A later study by McKinstry *et al.* presented the synthesis of MOF-5 in a CSTR at atmospheric pressure obtaining the desired quality and with a STY of 1000 kg m<sup>-3</sup> day<sup>-1</sup> (see Fig 9c).<sup>155</sup>

### 3. Downstream processes

After any MOF synthesis, careful processing is required to obtain the final functional material. Directly after the synthesis, the product slurry needs to be washed with the reaction solvent to remove any unreactants and by-products, e.g. using a centrifuge or a Buchner filter. Subsequently, an activation process is required to remove guest molecules, trapped within the framework, to obtain the expected surface area of the structure. Depending on the MOF structure, these two stages can be the most time-limiting stages of the process and become hugely significant in the large-scale production. The last stages of the process consist in drying and shaping the MOFs as well as a heat activation step before testing. Figure 10 shows a diagram of the typical downstream processes for the synthesis of a MOFs.

- Insert Figure 10 -

Despite promising advances in MOF synthesis, there are still challenges remaining related to the downstream processing. On the laboratory scale these processes are well established and sufficient to obtain milligram of quality materials. For larger scale production, however, these conventional downstream methods are not well-suited to high production rates. The first stage, the washing and separation of the small crystals from the mother liquid still is a major obstacle for the large scale production MOFs. There are many well established types of equipment for solid-liquid separation such as centrifuges, cyclones, settling chambers, classifiers or filters, in addition to the direct evaporation of the mother liquor. However, the small size of the MOF particles, their low concentration in the solvent, as well as their density approaching that of the solvent (due to the high porosity), makes separation via most conventional methods inefficient or expensive at an industrial scale.<sup>156</sup>

Once the MOF slurry has been cleaned of the excess linkers and by-products, the activation stage is the next step of the process in order to obtain the highest porosity and BET surface area of the framework. Several strategies exist to remove the unreactants and solvent molecules trapped in the pores of the MOFs without collapsing the framework.<sup>157</sup> The most common procedure is a simple heating of the MOF to certain temperature under vacuum. Each MOF has its optimal protocol in order to obtain the highest surface area but generally the temperature should be between the boiling point of the solvent and the decomposition temperature of the structure. However, in most cases this strategy leads to a lower surface area, or to a collapse of the structure due to the high surface tension

and capillary forces imposed on the structure by the liquid-gas phase transition of the trapped solvent molecules. An alternative strategy to exchange the solvent used for the synthesis with one that has a lower-boiling point such as methanol, chloroform or acetone prior to heating the sample under vacuum. This strategy is laborious as generally most MOFs require soaking for a long period of time to ensure that the new solvent infiltrates. For example, in the case of MOF-74 and UiO-66 both MOFs require a soaking in daily refreshed methanol for 3 and 7 days respectively to ensure the complete removal of DMF (solvent used for the synthesis and washing stage) from the pores.<sup>36,158</sup> Some frameworks, such as ZIF-8 and MIL-53 (Al) require a solvent exchange process with methanol with an additional thermal treatment, 300 °C for 2 hours and 330 °C for 72 hours to obtain the BET surface areas of 1630 m<sup>2</sup>.g<sup>-1</sup> and 1590 m<sup>2</sup>.g<sup>-1</sup>, respectively.<sup>31,159</sup>

An attractive substitute for the solvent exchange method is the use of supercritical CO<sub>2</sub>. This relatively new strategy consists of exchanging the synthetic solvent for a one that is miscible with liquid CO<sub>2</sub> such as ethanol or methanol and then subsequently exchanging this second one for liquid CO<sub>2</sub> at high pressure and temperature for several hours. The difference here is that the CO<sub>2</sub> supercritical phase eliminates surface tension and capillary forces making this activation method much milder than the conventional and solvent exchange methods. There are several MOFs that have been effectively activated with this strategy. For example, MOF-200 and MOF-210, where a simple solvent exchange followed by pore evacuation under vacuum was not effective, were successfully activated, without losing the porosity, by a full solvent exchange with liquid CO<sub>2</sub>.<sup>4</sup> The surface areas obtained were 4530 and 6240 m<sup>2</sup>.g<sup>-1</sup>, respectively. Another example is the supercritical CO<sub>2</sub> activation of bio-MOF-100 where the DMF solvated samples were soaked in ethanol for 48 hours, and an exchange/activation with CO<sub>2</sub> liquid over a period of 8 hours yielded a BET surface area of 4300 m<sup>2</sup>.g<sup>-1</sup>.<sup>160</sup> In a variant of this method the sample is placed in a column and the supercritical CO<sub>2</sub> flows through the sample instead of using static CO<sub>2</sub> exchange. This method was presented by Koh and co-workers who activated UMCM-9 microporous coordination polymers via supercritical CO<sub>2</sub> flow activation yielding a surface area BET of 4970 m<sup>2</sup>.g<sup>-1</sup>.<sup>161</sup>

Latter novelties on the activation have been based on freeze-drying activation techniques which uses thermal cycling and the vacuum sublimation of solvents (benzene and cyclohexane) at low temperatures to avoid the impact of capillary forces on porous structures in order to control the frameworks stability and improve its porosity.<sup>162</sup> Recently Rubio-Martinez *et al.* presented for the first time the use of megasonics as an alternative strategy for the simultaneous separation and activation of MOF crystals.<sup>163</sup> Its operating principle is based on the application of high frequency ultrasound to the MOF solution, leading to the separation of the solid MOF particles from the solvent. Additionally, the megasonic treatment leads to an activation a simultaneous removal of occluded reagents of the MOFs crystal. This one-step process showed an improvement of up to 47% the surface area of the final product and compared to conventional methods. The method removes one stage from the downstream processing and is readily scalable and thus capable of producing commercially usable product at a large scale.

Shaping of MOF powders produced in any of the fabrication methods explained above is also mandatory for using them in real industrial applications. For instance, extruded or compact MOFs in the form of beads, pellets and monolithic bodies are required if MOFs want to be used for gas separation and storage applications. In methane storage (*e.g.* Adsorbed Natural Gas or ANG), for example, it is utmost important to fill the storage tanks with the largest amount of adsorbent; a condition that can only be achieved if MOF powders are highly packed. Furthermore, powdered MOFs are usually more difficult to be handled and can potentially contaminate pipes



during charge/discharge cycles. For other applications such as functional textiles,<sup>164</sup> alternative shaping and/or integration methods that process MOFs into paper sheets,<sup>165</sup> fibers<sup>166</sup>, membranes,<sup>167,168</sup> foams<sup>169</sup> or coatings<sup>170</sup> are also needed (Figure 11).

**- Insert Figure 11-**

Considering the potential adsorption-related applications of MOFs, most of the efforts done in shaping MOFs have been dedicated to their densification. The objective of densification is to pack the maximum amount of an active MOF on a certain volume without losing its integrity and adsorption capacity. Dailly *et al.* calculated that doubling the density of HKUST-1 powder would result in an adsorbent with performances comparable of those of the state-of-the-art carbons at intermediate pressures (30-100 bars).<sup>171</sup> However, despite the high industrial importance of shaping MOF powders, the interest of academic research groups to face this problematic is quite recent. In fact, the structuration of MOFs into shaped bodies was initiated by some companies (mainly, BASF), which tend to keep these shaping processes as in-house know-how or are only disseminated in patents. In this context, BASF published the first patent application concerning “shaped bodies containing metal-organic frameworks” in 2002. This patent was centered in the fabrication of MOF-2 and MOF-5 pellets using an eccentric press. In this process, both MOFs were mixed with graphite that acts as a binder improving their mechanical strength.<sup>172</sup>

Pelletization under pressure is probably the most common method used for densifying MOFs. In this process, a fine powder is pressed at a certain pressure to give pellets that can be crushed or fractionized by sieving. In some cases, before MOF powder is pressed, it can be blended with a binder to improve the cohesion between crystals and their mechanical strength. There are however two factors of this method that tend to affect the final adsorption properties of the pellet shaped MOFs. From one side, the pressure applied can crush the structure of the MOF due to its low mechanical stability. From the other side, the use of binders can dilute the porous powder and/or cause pore blockage, resulting in a reduced performance per unit mass (or volume) of the adsorbent.

As shown in Table 4, the influence of the pressure applied during pelletization of MOF powders was studied in some representative MOFs. However, systematic studies that correlate the pelletization conditions with the resulting adsorption properties of MOFs are very limited, and some discrepancies can be found. A general tendency when compressed pellets are processed is a decrease of the BET surface area and porosity of MOFs. This is specially the case for HKUST-1 that is mechanically fragile. For HKUST-1, it has been described that a significant loss of its BET surface area occurs at moderate pressures. Ahn *et al.* reported a loss of 50 % of its BET surface area when the applied pressure was around 10 MPa,<sup>173</sup> whereas Bazer-Bachi *et al.*<sup>174</sup> and Peterson *et al.*<sup>175</sup> found a similar decrease when pressures of 80 MPa and 70 MPa were applied, respectively. Other MOFs have shown better mechanical resistance. For example, UiO-66 and analogues, which are known for their high mechanical and thermal stability owing to their 12-fold connected clusters in the three spatial directions, were shown better stability during the compression process. Here, Peterson *et al.* observed a loss lower than 10 % of the BET surface area of UiO-66 when it was pelletized under a pressure of 70 MPa.<sup>175</sup> Dietzel *et al.* also reported the total conservation of the BET surface area of CPO-27 after tableting it at 100 MPa, whereas its porous character totally disappears at 1GPa.<sup>176</sup> In the case of ZIF-8, the BET surface area was well preserved until a pressure of 700 MPa. Above this pressure, different reports revealed some discrepancies. While Bazer-Bachi *et al.* observed

a loss lower than 20 % of its BET surface area,<sup>174</sup> Chapman *et al.* observed a loss of 50 % at pressures above 1 GPa.<sup>177</sup> This difference can be attributed to non-reported parameters, such as the pressure increase rate and the dwell time, which can dramatically influence the integrity of the final pellet.

#### Insert Table 4

Binders are sometimes utilized during this pelletization process. As state above, they basically serve to improve the cohesion between MOF crystals and their mechanical stability. Some tested binders include graphite,<sup>178</sup> polyvinyl alcohol (PVA)<sup>179</sup> and cellulose ester.<sup>174</sup> To our knowledge, however, there is no a systematic, rational study on the influence of the nature and concentration of these binders on the BET surface area and general properties of MOFs during their pelletization.

The presence of binders is also necessary in other shaping processes, including foaming, extrusion, granulation and cake crushing. In all these procedures, MOF powders are initially dispersed in a solvent/binder mixture. The choice of the binder gives a certain texture and property to the mixture, which is then manipulated in different ways to obtain the desired MOF shapes. For example, in the extrusion process, the MOF solvent/binder mixture forms a paste that can then be extruded to induce shaping of the MOF into different morphologies (Table 4). Following this latter method, Kaskel *et al.* mixed HKUST-1 crystals with a silicone resin and a plasticizer to form a paste that was subsequently extruded into monolithic HKUST-1 strings in a ram extruder. In this case, the decrease of the BET surface area was significant (70% of its initial BET surface area) due to the presence of binders and heating conditions, but the performance of the extruded monolith was higher than the monolith obtained by *in situ* synthesis of HKUST-1 in cordierite honeycombs.<sup>180</sup> The extrusion method was also used by Ren *et al.* to prepare UiO-66 spherical pellets (with a BET surface area of 674 m<sup>2</sup>.g<sup>-1</sup> that corresponds to 50 % of its initial value) from a paste made of UiO-66 and 10 wt.% sucrose/H<sub>2</sub>O mixture using a granulator.<sup>181</sup>

Starting from the binder-solvent-MOF mixture, monolithic MOF foams can also be formed (Table 4). In this case, the nature of the binder tends to form macroporous foam-type solids in which the MOF can be entrapped. Similar MOF foams can also be produced by synthesizing the MOF in the presence of pre-formed foam. Using both approaches, foams with MIL-101,<sup>182</sup> HKUST-1<sup>183</sup> and UiO-66<sup>184</sup> were prepared. For example, Wang *et al.* synthesized a foam monolith composed of HKUST-1@Fe<sub>3</sub>O<sub>4</sub>-MF (MF means magnetic fluid) by dispersing HKUST-1@Fe<sub>3</sub>O<sub>4</sub>-MF particles in an aqueous carboxymethylcellulose solution. The treatment with acetonitrile and posterior drying let to the formation of monolithic foams with high catalytic activity for C-H oxidation.<sup>185</sup>

Other shaping processes require the formation of a dried MOF cake that is crushed. Here, the MOF powder is mixed with a certain amount of a binder (typically, polyvinyl alcohol (PVA)) and the resulting mixture is dissolved in a solvent forming a paste. This paste is then dried, crushed and sieved into the wanted particle size fraction. Denayer *et al.* used this method to prepare MIL-53(Al) pellets using PVA as the binder. As revealed by N<sub>2</sub> adsorption isotherms, the MIL-53(Al) pellets showed a loss of BET surface area of 32 % but maintained good CH<sub>4</sub>/CO<sub>2</sub> selectivity capacities.<sup>179</sup> Finally, other methodologies have also started to be explored to incorporate MOFs into fibers<sup>186</sup> and papers, and shape them into alginate-based spherical beads<sup>187</sup> or ceramic beads.<sup>188</sup>

With this few examples, it is obvious that the shaping of MOFs for specific applications is still in an embryonic stage and strong efforts have still to be dedicated to the rational study of this process if we want to be able to access to the real commercial applications. It is also clear that, in adsorption-related applications, this shaping

process must respect the relatively low thermal, chemical and mechanical stability of MOFs so that their adsorption capacities are mostly preserved. For other applications, however, this latter condition should not be so important. In catalysis, for example, Bazer-Bachi *et al.* observed that, even though pelletization of ZIF-8 decreased its adsorption properties, it did not change its catalytic activity.<sup>174</sup>

#### 4. Perspectives and commercial developments

Since the first patent filed in 1995 and assigned to the Nalco Chemical Company, commercialisation of MOFs progressed gradually until the first MOF-based products released in 2016 by MOF Technologies and Numat Technologies (see Figure 12).<sup>189,190</sup> MOF production at scale is now underway which will help secure customer confidence and open the door for other MOF-based products. However, the growing market will push the MOF suppliers for further cost-efficiency, reproducibility and environment sustainability to remain competitive. Here is a brief summary of companies working with MOFs in production, technology development and retail to date.

- Insert Figure 12 -

MOF Technologies was founded in 2012 based on patented mechanochemical manufacturing technology invented at the Queen's University of Belfast.<sup>47</sup> This innovative process allows the production of MOFs using little or no solvents. Solvent-free synthesis has advantages in both waste and energy management. Solvent waste is a major issue in the chemical industry. The energy required to initiate reaction can sometimes be reduced using mechanical energy rather than thermal energy. Recently this method has been configured for continuous production through extrusion which is scalable.

It is unknown how many MOFs can be manufactured using mechanochemical synthesis, however MOF Technologies offer a wide catalogue for direct purchase. At the end of 2016 they sold around 100 kg of MOFs from their catalogue: Magnesium formate, Cu-BTC (HKUST-1), ZIF-8, Al(OH) Fumarate, ZIF-67, Mg-MOF-74 and Zn-SIFSIX-Pyrazine. See Table 5 for summary of MOFs for sale from each manufacturer.

MOF Technologies were the first to announce a MOF-based commercial product available through fruit and vegetable supplier Decco Worldwide Post-Harvest Holdings. The product has been registered with the U.S. Environmental Protection Agency under the proprietary name NT-7815 (EPA reference: 2792-79). NT-7815 is described as a micro-adsorbent delivering 0.7 w.t% of 1-MCP, which is a gas that blocks postharvest ethylene responses, extending the storage life and quality of many fruits and vegetables. MOF Technologies has not released any details regarding the MOF incorporated within the product. With the announcement of the new product, MOF Technologies have expanded their production facility capable of producing 15 kg/h in preparation for full scale between 5 and 10 tonnes per year from 2018 depending on which MOF.<sup>191</sup>

-Insert table 5 -

NuMat Technologies established in 2013, have also released a MOF-based product called ION-X based on a proprietary set of MOFs for storing gases such as arsine, phosphine and boron trifluoride for the electronics industry.<sup>192</sup> The company is setting up a facility in Asia that will receive MOF-filled tanks from the United States. NuMat has a partnership with one of the top gas companies in Asia who will pump the tanks with gas which will then be distributed to customers. Asia also contains most of the major manufacturers of electronics in the world and therefore this position will likely offer direct access to this market which is 70% of the total demand. NuMat will lead the initial production of the proprietary set of MOFs for ION-X and have explored multiple manufacturing methods including flow, mechanochemical, solvothermal and others.

MOF Apps, founded in 2013, are the exclusive licensee for UiO-66 and the zirconium-based family of MOFs. With a focus on MOF Application Services, the company aims to bring research and industry together to identify and develop commercially viable application opportunities in the areas of gas storage, industrial cooling, toxic gas protection and healthcare. MOF Apps develops and offers integrated solutions using MOFs which are cost-competitive and which outperform state-of-the-art systems. MOF Apps have sold the most amount of MOF to a leading vehicle manufacturer in August 2015 to test as adsorbed natural gas fuel platform.<sup>193</sup>

ProDia is a Horizon 2020 project funded through the European commission. It is a consortium of over 15 parties focused on the development of reliable production methods of nanoporous materials and their applications. Pilot-scale production of up to 100 kg will be led by Johnson Matthey for water-based synthesis, MOF Technologies for mechanosynthesis and Axel One for spray-drying synthesis.<sup>194</sup>

ProfMOF founded in 2015 by a group of scientists at the University of Oslo, Inven2 and Kongsberg, focused on the commercialization of the MOF-material. ProfMOF prefer water-based and continuous flow production of MOFs. Prof Norbert Stock, inventor of CAU series and advisor for ProfMOF, has developed the water-based synthesis method for some of the zirconium MOFs and CAUs series.<sup>43,195,196</sup> The ProfMOF catalogue includes: CAU-10, UiO-66, UiO-66-ADC, UiO-66-FA, UiO-66-BDC, UiO-66-BDC-NH<sub>2</sub>, UiO-66-BDC-COOH and UiO-66-BPDC/UiO-67.<sup>197</sup>

STREM Chemicals Inc. has become a distributor of MOFs manufactured in agreement with various MOF companies including KRICT, Inven2 and Framergy. Their catalogue includes: (CuI)<sub>4</sub>(DABCO)<sub>2</sub>, (CuI)<sub>4</sub>(C<sub>6</sub>H<sub>14</sub>N<sub>2</sub>)<sub>2</sub>, C<sub>6</sub>H<sub>12</sub>N<sub>4</sub>(CuCN)<sub>5</sub>, PCN-250(Fe) CONEKTIC™ F250 by Framergy, MIL-100(Fe) KRICT F100 by KRICT, ZIF-8 and UiO-66 by Inven2.<sup>198</sup>

Sigma-Aldrich is a distributor of MOFs supplied by BASF under the product names Basolite® and Basosiv™. Figure 13 shows the total number of academic publications that reference these products. The actual number of sales or quantities is unavailable and therefore these numbers represent the minimum. According to this data, Sigma-Aldrich has made at least a total of 1198 sales for research purposes. Their catalogue includes: Cu-BTC Basolite® C300 by BASF, MIL-53 Basolite® A100 by BASF, Fe-BTC Basolite® F300 by BASF, ZIF-8

Basolite® Z1200 by BASF, MOF-177 Basolite® Z377 by BASF, Mg-Formate Basosiv™ M050 by BASF and Al-fumarate Basolite® A520 by BASF (no longer available).<sup>199</sup>

### **-Insert Figure 13-**

Pseudo-startup MOFWORX from CSIRO Australia is commercializing MOFs based on patented flowchem manufacturing technology together with a diverse material and application-based portfolio. The group have built a reactor called Mindi (the aboriginal name for a mythological serpent that spits out white powder) that is capable of 10 kg/h production. The company aims to become a product development house for MOF-based technologies supported by their own manufacturing capability.<sup>200</sup>

Other companies are working towards the commercialization of MOFs such as the MOFcompany, MOFGen, Framergy, ACSYNAM and Promethean particles.<sup>201–204</sup> MOFGen are developing nanoporous materials for materials for a number of applications including medical devices, wound-healing and consumer healthcare. Framergy own the license for PCN-250 which can be used for natural gas capture and storage, and currently sold through STREM Chemical Inc. Promethean Particles have commissioned a continuous flow reactor based on super critical water capable of producing 1,000 tonnes per year. The company has focused on nanoparticle production for inks electronics industry but are capable of shifting to MOF production if the market becomes more attractive.

## **5 Conclusions and Future priorities**

The last two decades have seen great progress in the field of Metal Organic Frameworks both in the discovery of new structures and the development of new functional properties of these nanomaterials. However, a crucial prerequisite for accessing this potentiality in real world applications is the ability to routinely synthesise these materials in large quantities with high efficiency. It is only within the last five years that interest has arisen in the scientific community to develop novel synthetic methods and explore the scale up the synthesis of MOFs, focusing on economically viable strategies that do not rely on expensive or rare raw materials and also consider safety and environmental issues.

In this review, the advances in several synthetic methodologies were discussed. These new synthetic methods allow an unprecedented level of control over the reaction conditions, which in turn lead to a better control over particle size morphology, and reproducibility between batches. However, there are still a few issues remaining before MOF production reaches the level of a mature commercial technology. The solvent free approach and water-based synthesis are the most likely strategies to succeed in becoming economically and environmentally feasible for large ton scale production. Aside from the development of synthetic routes, another critical area is downstream processing, as the conventional downstream methods used at the laboratory scale are not well-suited to high production rates. This means that large scale application of MOFs will be limited by their commercial availability and thus most likely also the sustainability of the synthesis procedure until these methods are further

developed. This future research, which will involve researchers of many different fields, will certainly introduce metal–organic materials up to their use for real practical applications.

Efforts in MOF commercialization have lead to the creation of several spin off companies, and the two new MOF markets recently released open a new and exciting time.

## ACKNOWLEDGMENTS

M. R. M, M. R. H. and A. T. acknowledge the financial support from CSIRO Mineral Resources and Manufacturing business units. M. R. H. acknowledges FT13000345 for funding support. C. A., I. I. and D. M. acknowledge the financial support from MINECO-Spain through projects PN MAT2012-30994, 2014-SGR-80, EU FP7 ERC-Co 615954, and European Union’s Horizon 2020 research and innovation programme under grant agreement No 685727.

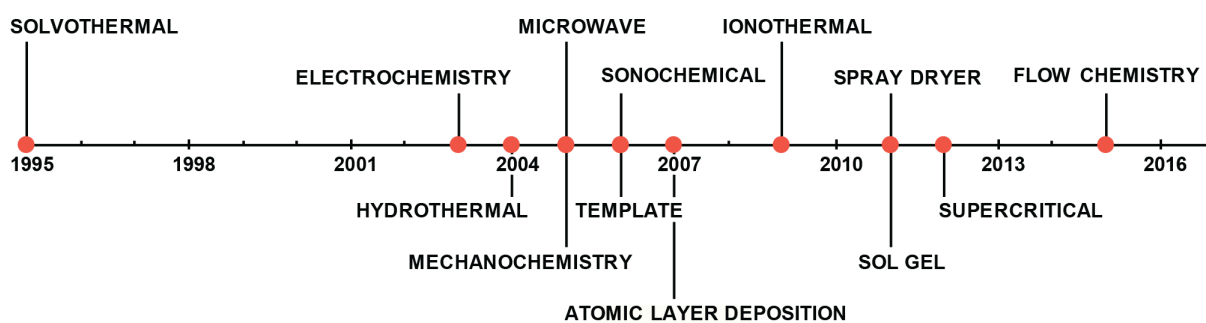
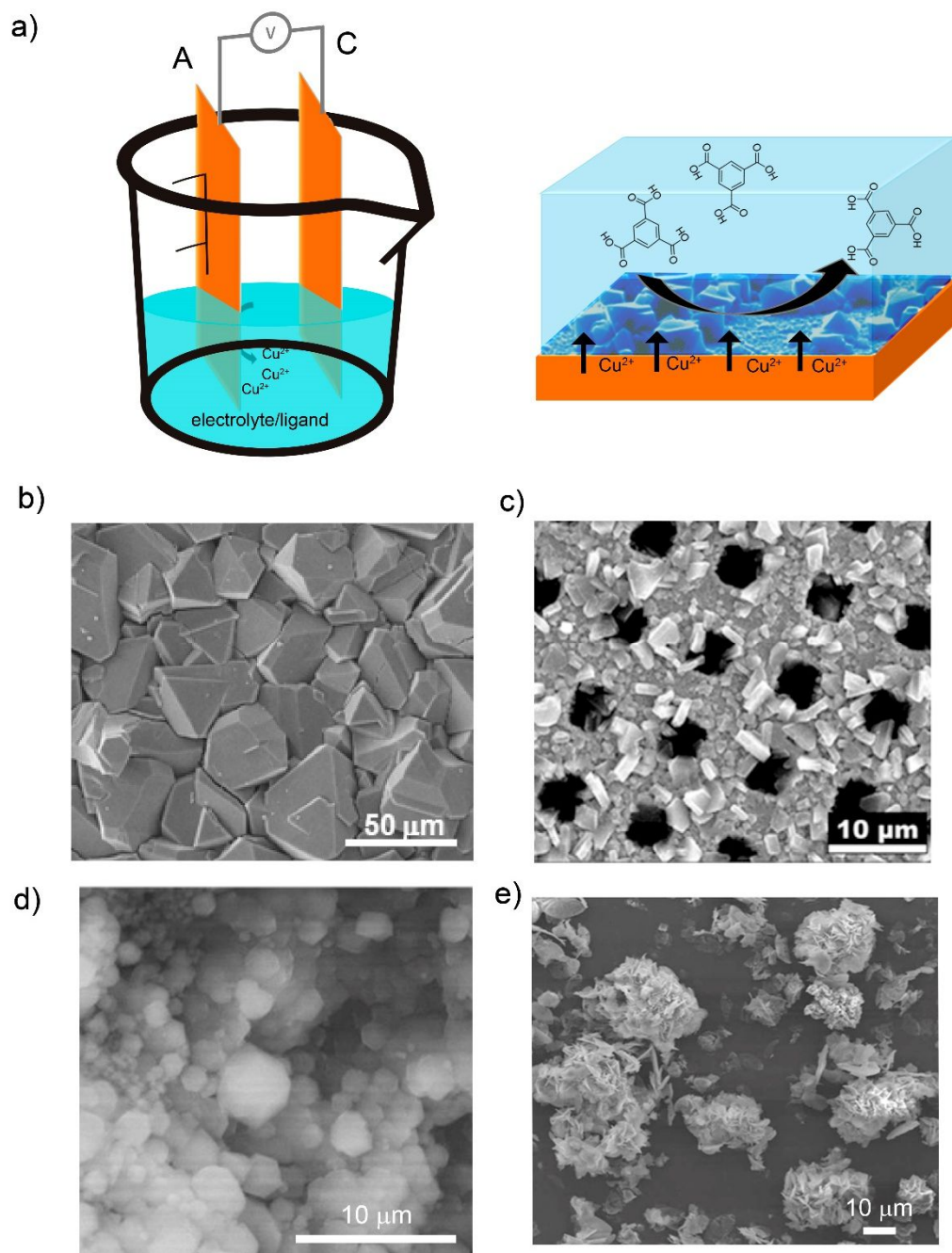
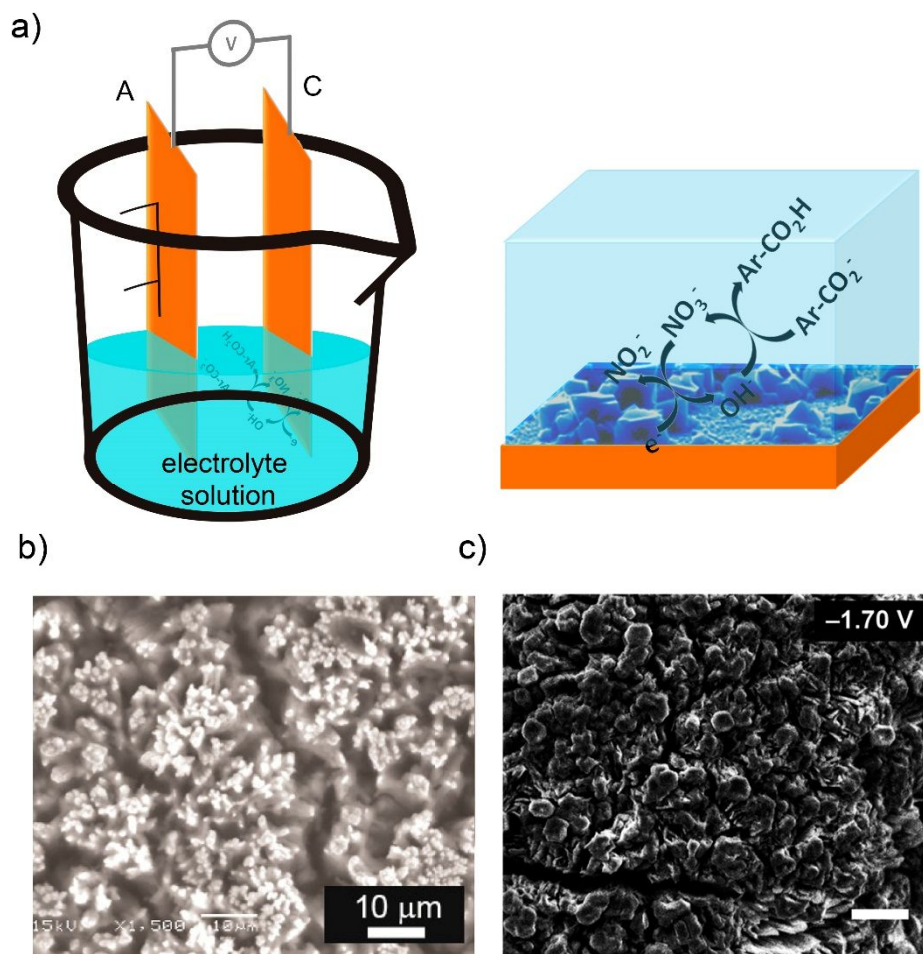


Figure 1: Timeline of the most common synthetic approaches patented for the synthesis of MOFs. <sup>28,45,46,48,49,205–210</sup>



**Figure 2: Electrosynthesis of MOFs by anodic dissolution.** a) Schematic illustration showing the anodic dissolution cell (right) and the formation of HKUST-1 on the anode electrode (left). b) SEM image of HKUST-1 on a copper electrode. c) SEM image of HKUST-1 on a copper mesh. d) SEM image of ZIF-8 particles on a zinc electrode. e) SEM images of flower-shaped MOF-5 on a zinc electrode. (© Elsevier, American Chemical Society and Royal Society of Chemistry, reprinted with permission from ref 57, 59, 65 and 68)



**Figure 3: MOF synthesis by cathodic deposition.** a) Schematic illustration showing the cathodic dissolution cell (left) and the reaction that takes place on the cathode electrode (right). b) SEM images of MOF-5 deposited on the cathode surface. c) SEM images of bilayer structures of MOF-5 and  $(\text{Et}_3\text{NH})_2\text{Zn}_3(\text{BDC})_4$ . (© Royal Society of Chemistry and American Chemical Society, reprinted with permission from ref 71 and 72)



**Table 1: Electrochemical synthesis of MOFs with different routes and conditions.**

<i>Anodic deposition</i>					
MOF	Substrates	Solvent	Electrolyte	BET surface area (m <sup>2</sup> ·g <sup>-1</sup> )	Ref.
HKUST-1	Copper electrode	MeOH	-	1820	50
	Copper electrode	EtOH:H <sub>2</sub> O	MTBS	-	57
	Copper mesh	EtOH: H <sub>2</sub> O	-	-	59
	Copper electrode	EtOH:H <sub>2</sub> O	MTBS	1440	58
	Copper electrode	EtOH: H <sub>2</sub> O, organic solvents	MTBS	-	61
	Copper mesh				
	Copper electrode	EtOH, EtOH: H <sub>2</sub> O	MTBS	1309	63
ZIF-8	Zinc electrode	AcN: H <sub>2</sub> O	MTBS	1600	58
	Zinc electrode	DMF:H <sub>2</sub> O	MTBS	1730	65
ZIF-4	Zinc electrode	DMF:H <sub>2</sub> O	MTBAMS	75	65
ZIF-14	Zinc electrode	DMF: H <sub>2</sub> O	MTBAMS	598	65
ZIF-7	Zinc electrode	DMF:H <sub>2</sub> O	MTBAMS	358	65
ZIF-64	Cobalt electrode	DMF: H <sub>2</sub> O	MTBAMS	1521	65
MIL-53(Al)	Aluminium electrode	DMF:H <sub>2</sub> O	KCl or NaCl	1200	58
MIL-100 (Al)	Aluminium electrode	EtOH: H <sub>2</sub> O	-	969	58
MIL-100 (Fe)	Iron electrode	EtOH:H <sub>2</sub> O	MTBS	-	64
Tb-BTC	Terbium foil	EtOH: H <sub>2</sub> O	MTBS	-	66
Gd-BTC	Gadolinium foil	EtOH:H <sub>2</sub> O	MTBS	-	66
MOF-5	Zinc plate	EtOH: H <sub>2</sub> O	NH <sub>4</sub> F	-	67
	Zinc plate and titanium plate	DMF	BMIM	914.7	68, 69

***Cathodic deposition***

MOF	Substrates	Method	Ref.
MOF-5	FTO	Cathodic	70
UiO-66	Zirconium foil	Anodic and cathodic	76
MOF-5	FTO	Cathodic	71
MOF-5 /(Et <sub>3</sub> NH <sub>2</sub> ) <sub>2</sub> Zn <sub>3</sub> ( BDC) <sub>4</sub>	FTO	Cathodic	72

***Others***

MOF	Substrates	Method	
ZIF-8	Zinc wire	BE	77
UiO-66	FTO	Electrophoretic deposition	74
HKUST-1	FTO	Electrophoretic deposition	73
	Glass	Galvanic displacement	75
	Porous stainless steel	Electrophoretic deposition	73
	Cu bead	BE	77
MIL-53	FTO	Electrophoretic deposition	74
NU-1000	FTO	Electrophoretic deposition	74

Abbreviations: MTBS, methyltributylammonium methyl sulfate; MTBAMS, methyltributylammonium methyl sulphate; BMIM, 1-butyl-3-methylimidazole; FTO, fluorine doped tin oxide; BE, bipolar electrochemistry.

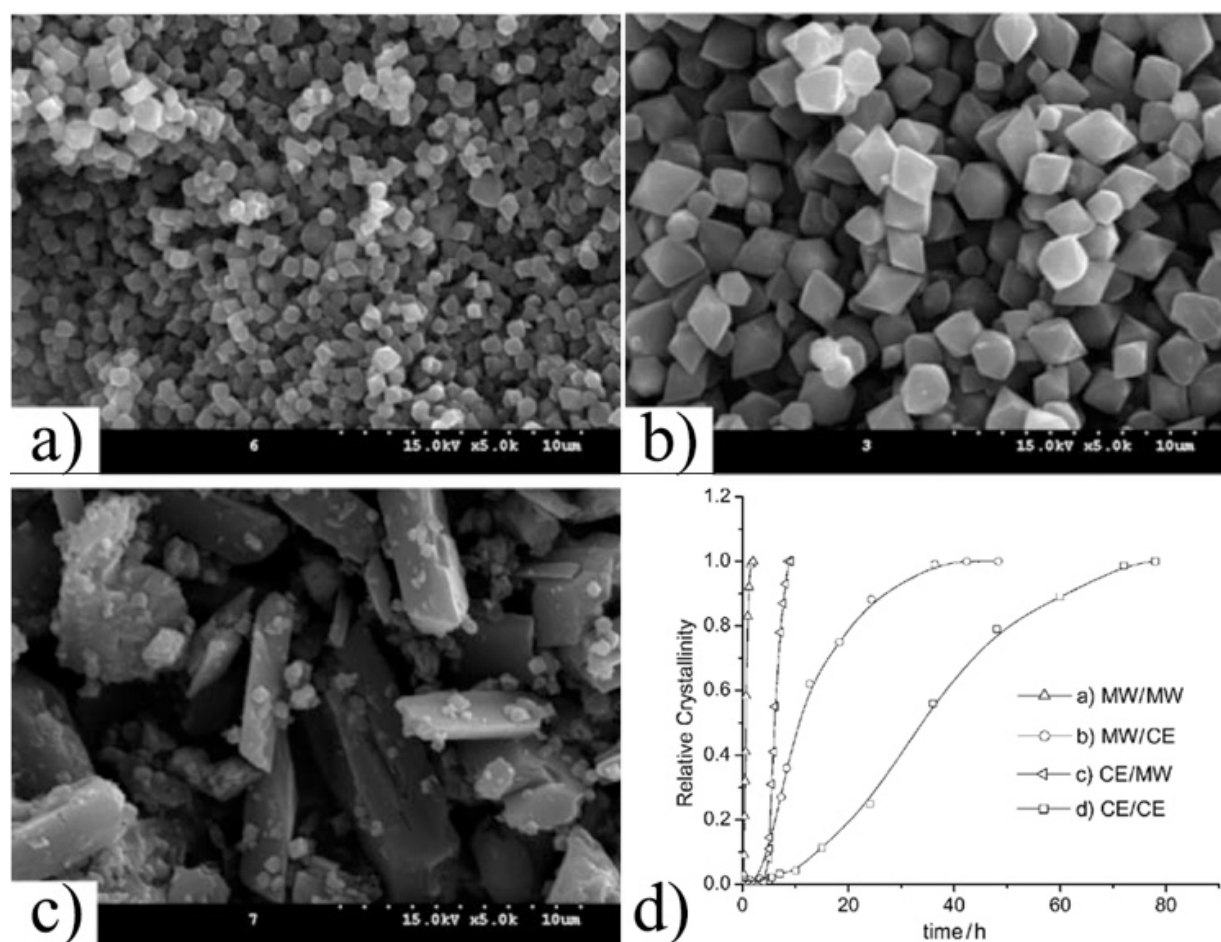


**Figure 4: SEM images of synthesis of MIL-53(Fe).** Synthesis at 70 °C with a) ultrasounds for 35 min, b) microwave for 2 h, and c) conventional electric heating for 3 days d) Comparison crystallization curves for the synthesis of MIL-53(Fe) in two steps by a) microwave, b) microwave and conventional electric heating, c) conventional electric heating and microwave and d) conventional electric heating.<sup>91</sup> (© Elsevier, reprinted with permission from ref 80).

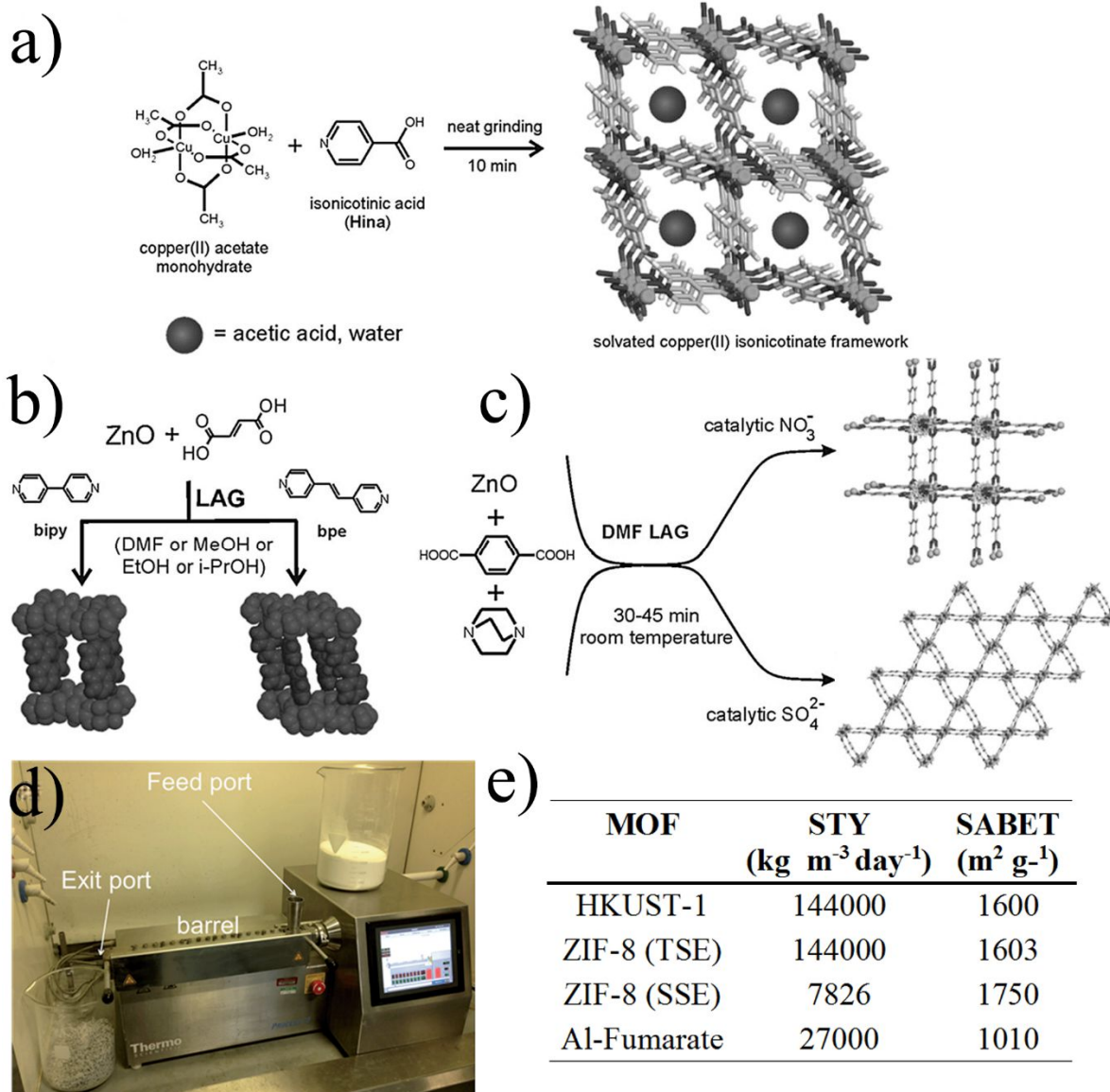


**Figure 5: Mechanochemical synthesis of MOFs.** a) neat grinding, b) liquid-assisted grinding c) ion- and liquid-assisted grinding, exploiting the catalytic effect of nitrates and sulphates d) twin screw extruder with key parts highlighted. e) Table of space time yields (STYs) and BET surface area for the synthesis of MOFs synthesized by extrusion methods (© The Royal Society of Chemistry, reprinted with permission from ref 106 and 107)

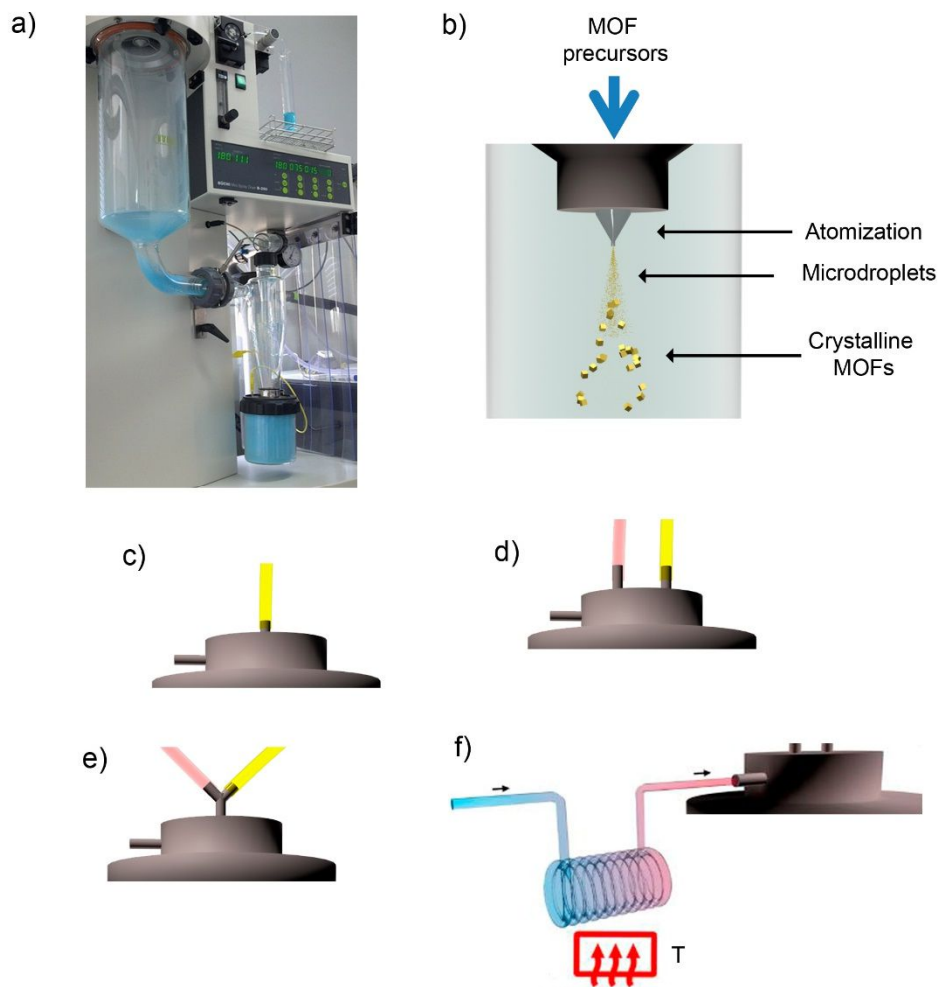


**Figure 6: Spray-drying method for the production of MOFs.** a) Photograph of the spray-dryer while it is used to fabricate HKUST-1. b) Schematic illustration of the spray-drying synthesis of MOFs. The MOF precursor solution can be introduced into the spray drier using a: c) two-fluid nozzle; d) three-fluid nozzle; e) T-junction; and f) continuous flow reactor coupled to a two-fluid nozzle. ((©Springer Nature and The Royal Society of Chemistry, adapted with permission from ref. 132 and 134).

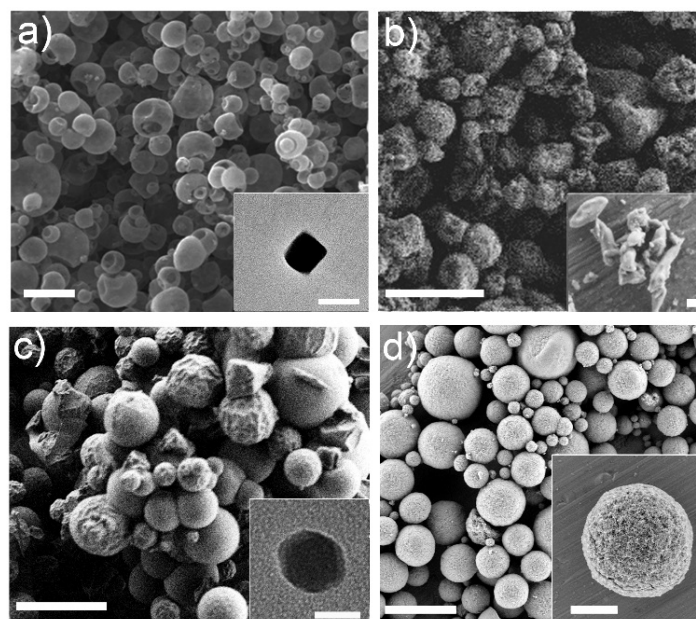


**Figure 7: SEM and TEM images of several MOFs synthesized by spray-drying.** a) Hollow spherical superstructures of HKUST-1 synthesized using a two-fluid nozzle. Inset shows a TEM image of a single HKUST-1 nanoparticle. b) Spherical superstructures of MIL-88A synthesized using a T-junction. Inset shows a SEM image of MIL-88A particles. c) Superstructures of ZIF-8 synthesized using a three-fluid nozzle. Inset shows a TEM image of a single ZIF-8 nanoparticle. d) Compact superstructures/beads of UiO-66 synthesized using a continuous flow reactor coupled to a two-fluid nozzle. Inset shows a SEM image of a single bead. Scale bars: 10  $\mu\text{m}$  (c), 5  $\mu\text{m}$  (a,d), 2  $\mu\text{m}$  (b, inset d), 200 nm (inset b), and 50 nm (inset a,c). (©Springer Nature and The Royal Society of Chemistry, reprinted with permission from ref 132, 134).

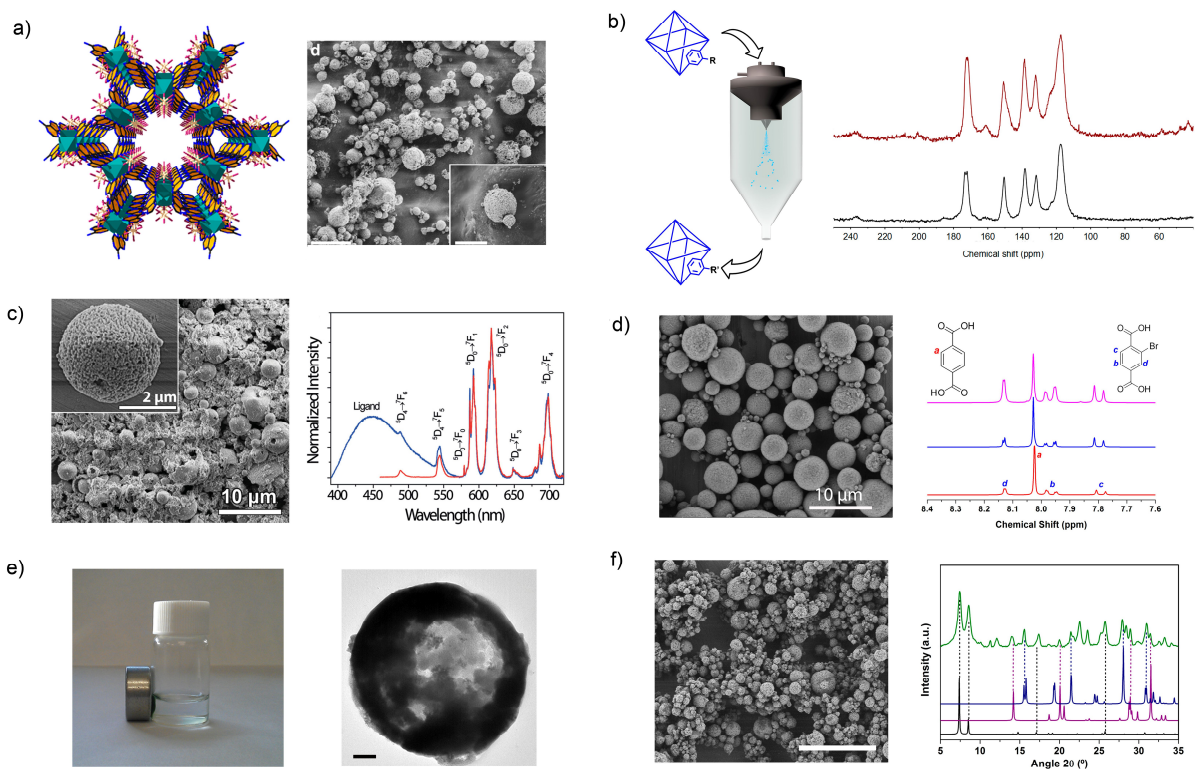


Figure 8: Spray-drying method for building and/or modifying MOFs. a) Crystal structure and SEM image of MPM-1-TIFSIX. Scale bar: 20  $\mu\text{m}$  and inset: 5  $\mu\text{m}$ . b) Schematic illustration of the post-synthetic modification of MOFs using spray-drying and  $^{13}\text{C}$  MAS-NMR spectra that confirms the formation of the CH=N imine group. c) SEM image of a multi-metallic lanthanide-based MOF and excitation spectra of it. Scale bar: 10  $\mu\text{m}$  and inset: 2  $\mu\text{m}$ . d) SEM image of a multi-variate UiO-66 and NMR spectra confirming that both BDC and BDC-Br are forming the UiO-66 structure. Scale bar: 10  $\mu\text{m}$ . e) HKUST-1 coupled with magnetic nanoparticles. Scale bar: 200 nm. f) SEM image of UiO-66 coupled with  $\text{CaCl}_2$  and XRD pattern of the composite material showing the presence of both components. Scale bar: 20  $\mu\text{m}$ . (©Springer Nature and The Royal Society of Chemistry, reprinted with permission from ref 132, 134, 135, 136, 137, 139).

**Table 2: MOFs synthesized by spray-dryer with different introducing modes and conditions.**

<i>Two fluid nozzle</i>							
<u>MOF</u>	<u>Metal salt/ Ligand/ Solvent</u>	<u>Feed rate (mL/min)</u>	<u>Inlet T (°C)</u>	<u>Yield (%)</u>	<u>BET (m<sup>2</sup>/g)</u>	<u>Ref.</u>	
HKUST-1	Cu(NO <sub>3</sub> ) <sub>2</sub> ·2.5H <sub>2</sub> O/ BTC/ DMF:EtOH: H <sub>2</sub> O	4.5	180	70	1260	132	
Cu-BDC	Cu(NO <sub>3</sub> ) <sub>2</sub> ·2.5H <sub>2</sub> O/ BDC/ DMF	4.5	180	70	543	132	
NOTT-100	Cu(NO <sub>3</sub> ) <sub>2</sub> ·2.5H <sub>2</sub> O/ BPTC/ DMF: H <sub>2</sub> O	4.5	180	54	1140	132	
MOF-14	Cu(NO <sub>3</sub> ) <sub>2</sub> ·2.5H <sub>2</sub> O/ BTB/ DMF:EtOH:H <sub>2</sub> O	4.5	180	30	-	132	
Zn-MOF-74	Zn(NO <sub>3</sub> ) <sub>2</sub> ·6H <sub>2</sub> O/ DHBDC/ DMF: H <sub>2</sub> O	4.5	180	50	-	132	
Mg-MOF-74	Mg(NO <sub>3</sub> ) <sub>2</sub> ·6H <sub>2</sub> O/ DHBDC/ DMF:EtOH:H <sub>2</sub> O	4.5	180	35	-	132	
Ni-MOF-74	Ni(NO <sub>3</sub> ) <sub>2</sub> ·6H <sub>2</sub> O/ DHBDC/ DMF:EtOH: H <sub>2</sub> O	4.5	180	40	-	132	
MIL-88B	FeCl <sub>3</sub> / 2-amino-BDC/ DMF:MeOH:H <sub>2</sub> O	4.5	180	27	-	132	
<i>Three fluid nozzle</i>							
<u>MOF</u>	<u>Metal salt/ Ligand/ Solvent</u>	<u>Feed rate (mL/min)</u>	<u>Inlet T (°C)</u>	<u>Yield (%)</u>	<u>BET (m<sup>2</sup>/g)</u>	<u>Ref.</u>	
ZIF-8	Zinc acetate/ MiM/ H <sub>2</sub> O	4.5	180	10	941	132	
Cu-PB	Cu(NO <sub>3</sub> ) <sub>2</sub> / K <sub>3</sub> Co(CN) <sub>6</sub> / H <sub>2</sub> O	4.5	180	20	617	132	
SIFSIX-3-Co	CoSiF <sub>6</sub> / Pyrazine/ MeOH	2.4	85	44	-	136	
SIFSIX-3-Ni	NiSiF <sub>6</sub> / Pyrazine/ MeOH	2.4	85	-	-	136	
SIFSIX-3-Cu	CuSiF <sub>6</sub> ·H <sub>2</sub> O/ Pyrazine/ MeOH	2.4	85	55	-	136	
SIFSIX-3-Zn	ZnSiF <sub>6</sub> ·xH <sub>2</sub> O/ Pyrazine/ MeOH	2.4	85	57	-	136	
SIFSIX-1-Zn	ZnSiF <sub>6</sub> ·xH <sub>2</sub> O/ 4,4'-bipyridine/ MeOH	2.4	85	40	1300	136	
TIFSIX-1-Cu	Cu(NO <sub>3</sub> ) <sub>2</sub> ·2.5H <sub>2</sub> O/ 4,4'-bipyridine/ MeOH	2.4	130	79	1650	136	
<i>T junction</i>							
<u>MOF</u>	<u>Metal salt/ Ligand/ Solvent</u>	<u>Feed rate (mL/min)</u>	<u>Inlet T (°C)</u>	<u>Yield (%)</u>	<u>BET (m<sup>2</sup>/g)</u>	<u>Ref.</u>	
MIL-88A	FeCl <sub>3</sub> / Fumaric acid/ DMF:MeOH:H <sub>2</sub> O	4.5	180	40	-	132	
MOF-5	Zinc acetate/ BDC/ DMF	4.5	180	60	1215	132	
IRMOF-3	Zinc acetate/ 2-amino-BDC/ DMF	4.5	180	70	-	132	
MPM-1-TIFSIX	TiF <sub>6</sub> (NH <sub>4</sub> ) <sub>2</sub> / Cu(NO <sub>3</sub> ) <sub>2</sub> ·2.5H <sub>2</sub> O/ H <sub>2</sub> O:MeCN	2.4	150	74	805	136	
<i>Continuous Flow</i>							
<u>MOF</u>	<u>Metal salt/ Ligand/ Solvent</u>	<u>Feed rate (mL/min)</u>	<u>T1(°C)</u>	<u>Inlet T (°C)</u>	<u>Yield(%)</u>	<u>BET (m<sup>2</sup>/g)</u>	<u>Ref.</u>
UiO-66	ZrCl <sub>4</sub> / BDC/ DMF: H <sub>2</sub> O	2.4	115	180	70	1106	134

UiO-66-NH <sub>2</sub>	ZrCl <sub>4</sub> / 2-NH <sub>2</sub> -BDC/ DMFH <sub>2</sub> O	2.4	115	180	67	752	134
UiO-66-NH <sub>2</sub>	ZrOCl <sub>2</sub> / 2-amino-BDC/ DMF: H <sub>2</sub> O	2.4	90	180	83	1150	212
UiO-66-NO <sub>2</sub>	ZrCl <sub>4</sub> / 2-nitro-BDC/ Acetic acid:H <sub>2</sub> O	2.4	115	180	62	679	134
UiO-66-Br	ZrCl <sub>4</sub> / 2-bromo-BDC/ DMF: H <sub>2</sub> O	2.4	115	180	68	527	134
UiO-66-(OH) <sub>2</sub>	ZrCl <sub>4</sub> / 2,5-dihydroxy-BDC/ DMF:H <sub>2</sub> O	2.4	115	180	81	401	134
UiO-66-acetamido	ZrCl <sub>4</sub> / 2,5-dihydroxy-BDC/ DMF: H <sub>2</sub> O	2.4	115	180	51	586	134
UiO-66-1,4-NDC	ZrCl <sub>4</sub> / 1,4-NDC/ DMF: H <sub>2</sub> O	2.4	115	180	45	431	134
UiO-66-2,6-NDC	ZrCl <sub>4</sub> / 2,6-NDC/ DMF:H <sub>2</sub> O	2.4	115	180	49	557	134
Fe-BTC/MIL-100	Fe(NO <sub>3</sub> ) <sub>3</sub> .9H <sub>2</sub> O/ BTC/ DMF	2.4	135	180	78	1039	134
Ni <sub>8</sub> (OH) <sub>4</sub> (H <sub>2</sub> O) <sub>2</sub> (L) <sub>6</sub>	Ni(CH <sub>3</sub> COO) <sub>2</sub> .4H <sub>2</sub> O/ 1H-pyrazole-4-carboxylic acid/ DMF: H <sub>2</sub> O	2.4	100	180	60	377	134

Abbreviations: BTC, trimesic acid; BDC, 1,4-benzenedicarboxylic acid; BPTC, biphenyl-3,3',5,5'-tetracarboxylic acid; BTB, 1,3,5-tris(4-carboxyphenyl)benzene; DHBDC, 2,5-dihydroxyterephthalic acid; DMF, dimethylformamide; EtOH, ethanol; MeOH, methanol; MiM, 2-methyl imidazole; NDC, naphthalenedicarboxylic acid.



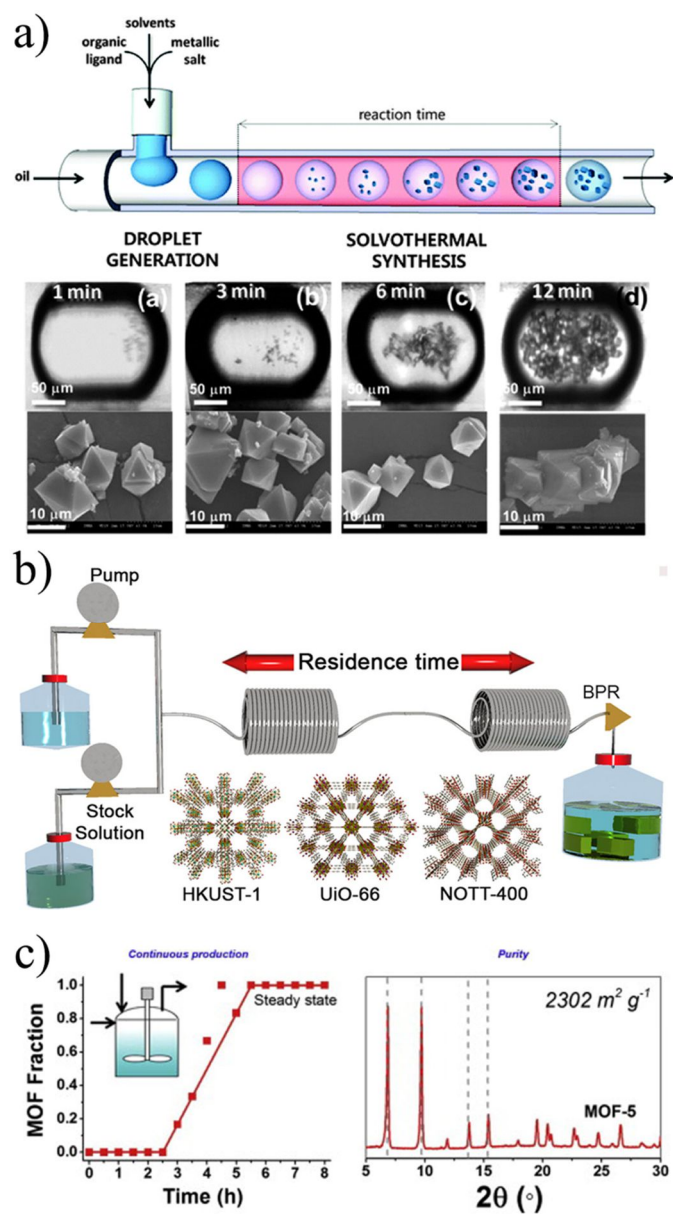


**Figure 9. Flow chemistry methods for the production of MOFs.** a) Schematic representation of a continuous flow microfluidic device for producing MOF crystals (top). Optical and SEM images of HKUST-1 crystals obtained *via* the microfluidic approach at different residence times. b) Schematic representation showing the continuous flow synthesis of HKUST-1, UiO-66 and NOTT-400 of MOFs. c) Reaction profile of the solvothermal synthesis of MOF-5 crystals with its corresponding x-ray pattern diffraction and BET surface area value. (© The American Chemical Society, Springer Nature and Elsevier, reprinted with permission from ref 141, 149 and 155)

**Table 3: MOFs synthesized by flow chemistry with different approaches and conditions.**

Method	MOF	Residence time	Temperature (°C)	STY (kg m <sup>-3</sup> day <sup>-1</sup> )	SA BET (m <sup>2</sup> g <sup>-1</sup> )
MF	HKUST-1 <sup>140</sup>	-	RT	-	620
	HKUST-1 <sup>141</sup>	1 min	90	5.8	1105
	MOF-5 <sup>141</sup>	3 min	120	-	3185
	IRMOF-3 <sup>141</sup>	3 min	120	-	2428
	UiO-66 <sup>141</sup>	15 min	140	-	1509
	MIL-88b <sup>137</sup>	4 min	95	-	-
	ZIF-8 <sup>143</sup>	15 s	RT	210000	1770
	Ce-BDC <sup>142</sup>	30 s	230	-	-
	UiO-66 <sup>144</sup>	0.44-2.2 min	120	-	922-1206
PFR	HKUST-1 <sup>149</sup>	1.2 min	85	4533	1805
	UiO-66 <sup>149</sup>	10 min	130	1186	672
	NOTT-400 <sup>149</sup>	15 min	85	1078	741
	Al-Fum <sup>150</sup>	1 min	65	97159	1054
	HKUST-1 <sup>148</sup>	5 min	60	-	1673
	MIL-53(Al) <sup>147</sup>	20 min	250	1021	919
	MIL-53(Al) <sup>147</sup>	20 min	250	1300	1010
	STA-12(Cd) <sup>151</sup>	5-20min	70	-	134
	ZIF-8 <sup>146</sup>	<5s	100	11625	1806
	ZIF-8 <sup>146</sup>	<5s	100	-	1780
	CAU-13 <sup>151</sup>	20 min	130	3049	401
	CPO-27 <sup>145</sup>	<5s	300	1501	1030
	HKUST-1 <sup>147</sup>	20 min	250	730	1554
	HKUST-1 <sup>145</sup>	<5s	300	4399	1950
	UiO-66 <sup>151</sup>	45 min	120	428	1263
	STA-12 <sup>151</sup>	20 min	70	428	134
	HKUST-1 <sup>153</sup>	1 min	360 W	64800	1550
	MIL-53(Al) <sup>153</sup>	4 min	200 W	3618	1376
	UiO-66 <sup>153</sup>	7 min	200W	7204	1052
	MOF74(Ni) <sup>152</sup>	<1s	150	2160	840
CSTR	UiO-66 <sup>154</sup>	8-40h	100-120	-	810
	MOF-5 <sup>155</sup>	5h	140	1000	2302

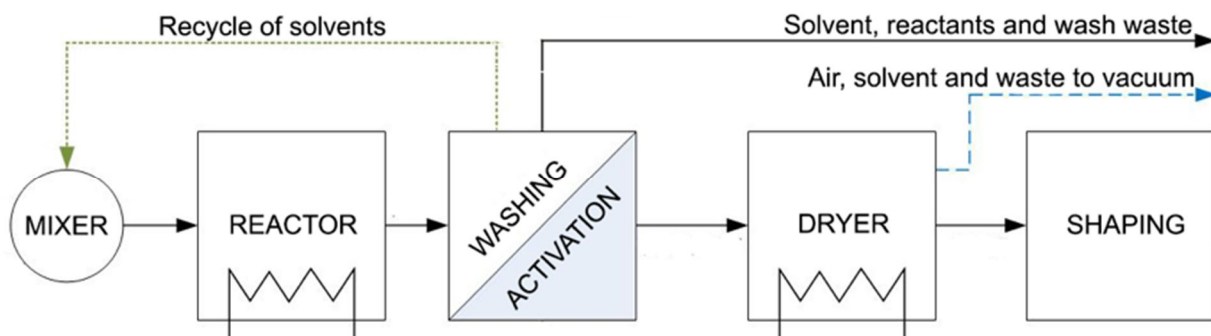


**Figure 10. Continuous MOF process.** Schematic representation of the different stages of the continuous process for MOFs production: synthesis, washing, activation, drying and shaping.

**Table 4: Examples of shaped MOFs using pelletization, foaming and extrusion methods.**

<i><b>Pellet</b></i>				
<u>MOF</u>	<u>Pressure</u>	<u>Binder</u>	<u>Property</u>	<u>Ref</u>
HKUST-1	-	Alox C and grahite	Very high adsorption capacity for CO <sub>2</sub>	178
	70 and 700 MPa	Without binder	50% decrease of the BET surface area (after 700 MPa)	175
	0.24 – 40 MPa	Cellulose ester, K15M	Maintained ammonia removal capacity 76% decrease of the BET surface area (after 40 Mpa)	174
	3-35 MPa	Without binder	50% decrease of the BET surface area (after 10 MPa)	173
MIL-53(Al)	1-8 bar	Polyvinyl alcohol	Below 5 bar, constant selectivity Above 5 bar, selectivity decreased. 22% decrease of the BET surface area	179
		Graphite	Suitable material for o-xylene over <i>p</i> - and <i>m</i> -xylene separation at low concentrations	214
UiO-66	-	Graphite	Maintained BET surface area	175
	70 and 700 MPa	Without binder	16% decrease in octane loadings (after 700 MPa)	174
ZIF-8	398-1432 Mpa	Cellulose ester, K15M	10% decrease of the BET surface area (after 1432 MPa) No change in catalytic reactivity	174
SIM-1	40-398 Mpa	Cellulose ester, K15M	28% decrease of the BET surface area (after 398 Mpa)	174
CPO-27-Ni	0.1-1 GPa	Without binder	Maintained methane storage capacity	176
<i><b>Foam</b></i>				
<u>MOF</u>	<u>Binder</u>	<u>Property</u>	<u>Ref</u>	
MIL-101 (Cr)	Ni foam	Decrease in hydrogen storage capacities (19%)	182	
UiO-66	Polyurethane	Maintaining more than 70% of the adsorption capacity for benzene and <i>n</i> -hexane	184	
UiO-66-NH <sub>4</sub> , Mg-MOF-74, HKUST-1, ZIF-8	Carboxymethylcellulose	-	185	
HKUST-1@Fe <sub>3</sub> O <sub>4</sub>	Carboxymethylcellulose	High catalytic activity in C–H oxidation	185	
<i><b>Extrusion</b></i>				
<u>MOF</u>	<u>Binder</u>	<u>Property</u>	<u>Ref</u>	
HKUST-1	Silres MSE 100 Culmial MHPC 20000 P	70% decrease of the BET surface area	180	
Zr-MOF	Sucrose and water	50% decrease of the BET surface area	182	

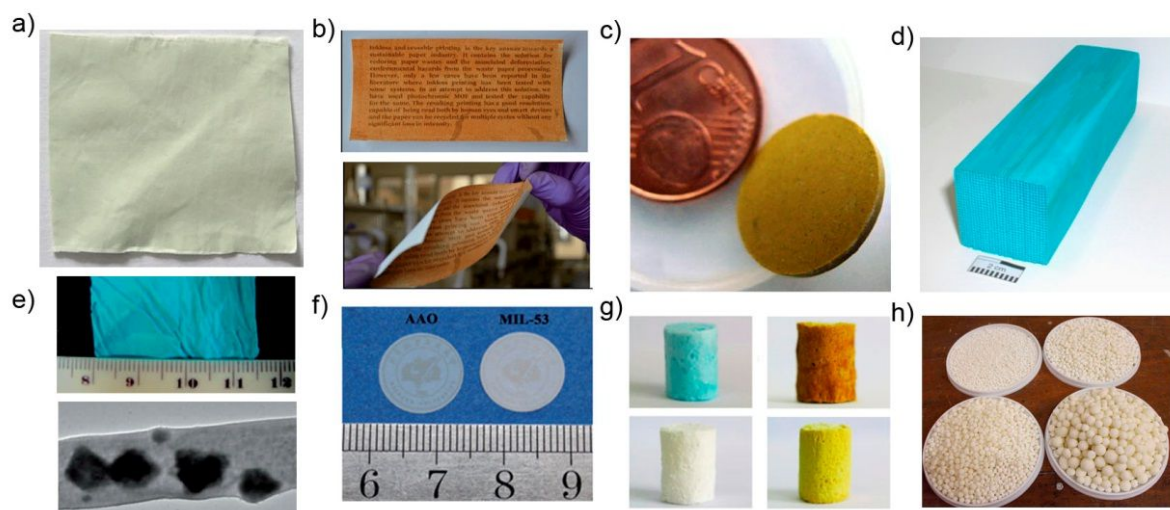


**Figure 11. Examples of shaped MOFs.** a) Functional textiles; b) Paper sheets; c) Pellets; d) Extruded monolith; e) Fibers; f) Membrane; g) Foams; and h) Granules. (© Nature Publishing group, American Chemical Society, Royal Society of Chemistry, Elsevier with permission from ref 163, 164, 165, 167, 180, 184)

**Table 5.** Sales catalogue of MOFs available by each manufacturer.

<b>MOF</b>	<b>Manufacturer</b>
Al(OH) fumarate	MOF Apps MOF Technologies
CAU-10	ProfMOF
Cu-BTC	BASF MOF Apps MOF Technologies
Fe-BTC	BASF
Magnesium formate	BASF MOF Technologies
Mg-MOF-74	MOF Technologies
MIL-100	KRICT MOF Apps
MIL-101-NH <sub>2</sub>	MOF Apps
MIL-53	BASF
MIL-68	MOF Apps
MOF-177	BASF
PCN-250(Fe)	Framergy
UiO-66 series	Inven2 MOF Apps ProfMOF
ZIF-67	MOF Apps MOF Technologies
ZIF-8	BASF MOF Apps MOF Technologies
Zn-SIFSIX-pyrazine	STREM Chemicals Inc. MOF Technologies

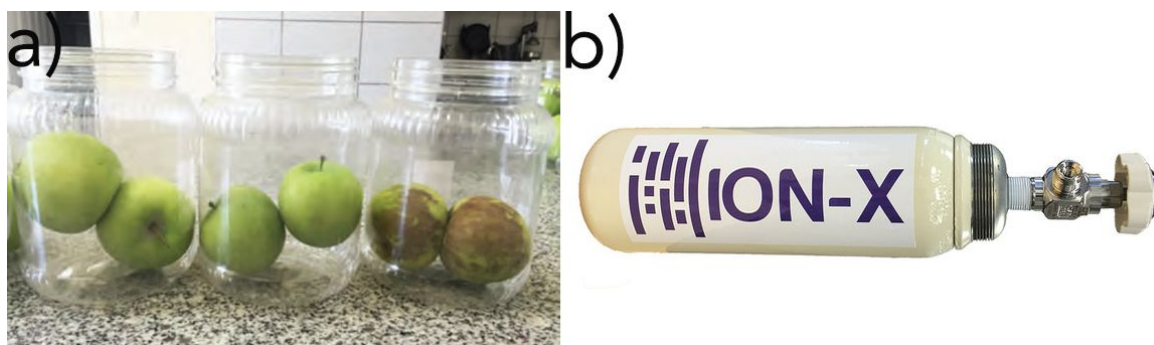


**Figure 12. Commercially available MOF-based products released in 2016.** a) NT-7815 micro-adsorbent for extending the storage life and quality of many fruits and vegetables by Decco Post-Harvest and MOF Technologies and b) ION-X gas storage tank for storing speciality gases used in the electronics manufacturing industry by Numat Technologies. (© The Springer Nature reprinted with permission from ref 191)

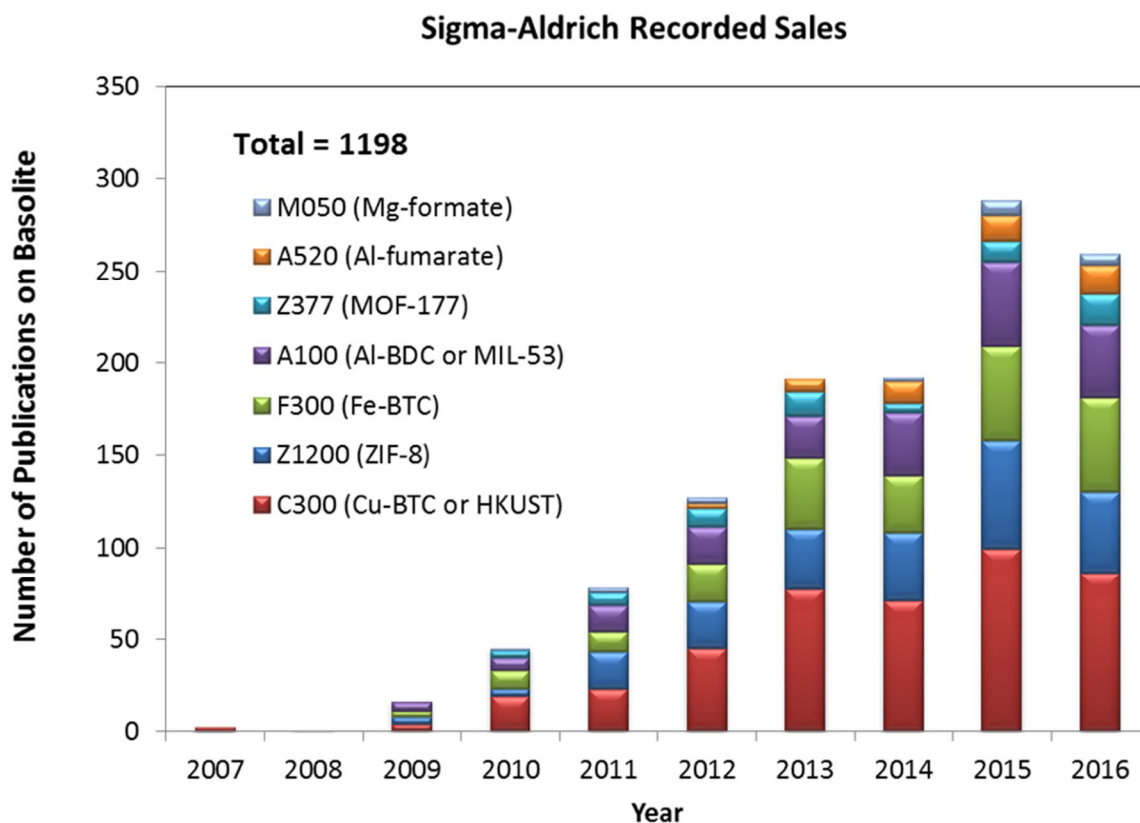


**Figure 13:** Number of publications referring to the Basolite® and Basosiv™ products supplied by Sigma-Aldrich.

## REFERENCES

1. Hoskins, B. F. & Robson, R. Infinite polymeric frameworks consisting of three dimensionally linked rod-like segments. *J. Am. Chem. Soc.* **111**, 5962–5964 (1989).
2. Hoskins, B. F. & Robson, R. Design and construction of a new class of scaffolding-like materials comprising infinite polymeric frameworks of 3D-linked molecular rods. A reappraisal of the zinc cyanide and cadmium cyanide structures and the synthesis and structure of the diamond-related frameworks  $[N(CH_3)_4][CuI ZnII(CN)_4]$  and  $CuI[4,4',4'',4''']$ -tetracyanotetraphenylmethane]BF<sub>4</sub>·xC<sub>6</sub>H<sub>5</sub>NO<sub>2</sub>. *J. Am. Chem. Soc.* **112**, 1546–1554 (1990).
3. Yaghi, O. M. & Li, H. Hydrothermal Synthesis of a Metal-Organic Framework Containing Large Rectangular Channels. *J. Am. Chem. Soc.* **117**, 10401–10402 (1995).
4. Furukawa, H. *et al.* Ultrahigh Porosity in Metal-Organic Frameworks. *Science* **329**, 424–428 (2010).
5. Kondo, M., Yoshitomi, T., Matsuzaka, H., Kitagawa, S. & Seki, K. Three-Dimensional Framework with Channeling Cavities for Small Molecules:  $\{[M_2(4, 4'$ -bpy)<sub>3</sub>(NO<sub>3</sub>)<sub>4</sub>·xH<sub>2</sub>O]<sub>n</sub> (M • Co, Ni, Zn). *Angew. Chem. Int. Ed. Engl.* **36**, 1725–1727 (1997).
6. Kitagawa, S., Kitaura, R. & Noro, S. Functional Porous Coordination Polymers. *Angew. Chem. Int. Ed.* **43**, 2334–2375 (2004).
7. Férey, G. *et al.* A Chromium Terephthalate-Based Solid with Unusually Large Pore Volumes and Surface Area. *Science* **309**, 2040–2042 (2005).
8. Serre, C. *et al.* Very Large Breathing Effect in the First Nanoporous Chromium(III)-Based Solids: MIL-53 or CrIII(OH)·{O<sub>2</sub>C–C<sub>6</sub>H<sub>4</sub>CO<sub>2</sub>}·{HO<sub>2</sub>C–C<sub>6</sub>H<sub>4</sub>–CO<sub>2</sub>H<sub>2</sub>. *J. Am. Chem. Soc.* **124**, 13519–13526 (2002).
9. Long, J. R. & Yaghi, O. M. The pervasive chemistry of metal–organic frameworks. *Chem. Soc. Rev.* **38**, 1213–1214 (2009).
10. McDonald, T. M. *et al.* Cooperative insertion of CO<sub>2</sub> in diamine-appended metal-organic frameworks. *Nature* **519**, 303–308 (2015).



11. Li, J.-R., Kuppler, R. J. & Zhou, H.-C. Selective gas adsorption and separation in metal–organic frameworks. *Chem. Soc. Rev.* **38**, 1477 (2009).
12. Kreno, L. E. *et al.* Metal–Organic Framework Materials as Chemical Sensors. *Chem. Rev.* **112**, 1105–1125 (2012).
13. Yi, F.-Y., Chen, D., Wu, M.-K., Han, L. & Jiang, H.-L. Chemical Sensors Based on Metal–Organic Frameworks. *ChemPlusChem* **81**, 675–690 (2016).
14. Liu, Y., Wang, Z. U. & Zhou, H.-C. Recent advances in carbon dioxide capture with metal-organic frameworks. *Greenh. Gases Sci. Technol.* **2**, 239–259 (2012).
15. Miller, S. R. *et al.* Biodegradable therapeutic MOFs for the delivery of bioactive molecules. *Chem. Commun.* **46**, 4526–4528 (2010).
16. Murray, L. J., Dincă, M. & Long, J. R. Hydrogen storage in metal–organic frameworks. *Chem. Soc. Rev.* **38**, 1294–1314 (2009).
17. A. Mason, J., Veenstra, M. & R. Long, J. Evaluating metal–organic frameworks for natural gas storage. *Chem. Sci.* **5**, 32–51 (2014).
18. Li, J.-R., Sculley, J. & Zhou, H.-C. Metal–Organic Frameworks for Separations. *Chem. Rev.* **112**, 869–932 (2012).
19. Voorde, B. V. de, Bueken, B., Denayer, J. & Vos, D. D. Adsorptive separation on metal–organic frameworks in the liquid phase. *Chem. Soc. Rev.* **43**, 5766–5788 (2014).
20. He, Y., Krishna, R. & Chen, B. Metal–organic frameworks with potential for energy-efficient adsorptive separation of light hydrocarbons. *Energy Environ. Sci.* **5**, 9107–9120 (2012).
21. D’Alessandro, D. M., Smit, B. & Long, J. R. Carbon Dioxide Capture: Prospects for New Materials. *Angew. Chem. Int. Ed.* **49**, 6058–6082 (2010).
22. Sumida, K. *et al.* Carbon Dioxide Capture in Metal–Organic Frameworks. *Chem. Rev.* **112**, 724–781 (2012).
23. Horcajada, P. *et al.* Metal–Organic Frameworks in Biomedicine. *Chem. Rev.* **112**, 1232–1268 (2012).

24. Horcajada, P. *et al.* Porous metal–organic-framework nanoscale carriers as a potential platform for drug delivery and imaging. *Nat. Mater.* **9**, 172–178 (2009).
25. Konstas, K. *et al.* Methane storage in metal organic frameworks. *J. Mater. Chem.* **22**, 16698–16708 (2012).
26. Prospects for Carbon Capture and Storage Technologies. *Annu. Rev. Environ. Resour.* **29**, 109–142 (2004).
27. Boot-Handford, M. E. *et al.* Carbon capture and storage update. *Energy Environ. Sci.* **7**, 130–189 (2013).
28. Yaghi, O. M. Novel crystalline metal-organic microporous materials. (1997).
29. Rabenau, A. The Role of Hydrothermal Synthesis in Preparative Chemistry. *Angew. Chem. Int. Ed. Engl.* **24**, 1026–1040 (1985).
30. Çolak, A. T., Pamuk, G., Yeşilel, O. Z. & Yüksel, F. Hydrothermal synthesis and structural characterization of Zn(II)- and Cd(II)-pyridine-2,3-dicarboxylate 2D coordination polymers,  $\{(NH_4)_2[M(\mu\text{-pydc})_2]\cdot 2H_2O\}_n$ . *Solid State Sci.* **13**, 2100–2104 (2011).
31. Loiseau, T. *et al.* A Rationale for the Large Breathing of the Porous Aluminum Terephthalate (MIL-53) Upon Hydration. *Chem. - Eur. J.* **10**, 1373–1382 (2004).
32. Deng, H. *et al.* Large-Pore Apertures in a Series of Metal-Organic Frameworks. *Science* **336**, 1018–1023 (2012).
33. McDonald, T. M. *et al.* Capture of Carbon Dioxide from Air and Flue Gas in the Alkylamine-Appended Metal–Organic Framework  $m\text{men-Mg}_2(\text{dobpdc})$ . *J. Am. Chem. Soc.* **134**, 7056–7065 (2012).
34. Cavka, J. H. *et al.* A New Zirconium Inorganic Building Brick Forming Metal Organic Frameworks with Exceptional Stability. *J. Am. Chem. Soc.* **130**, 13850–13851 (2008).
35. Valenzano, L. *et al.* Disclosing the Complex Structure of UiO-66 Metal Organic Framework: A Synergic Combination of Experiment and Theory. *Chem. Mater.* **23**, 1700–1718 (2011).

36. Katz, M. J. *et al.* A facile synthesis of UiO-66, UiO-67 and their derivatives. *Chem. Commun.* **49**, 9449 (2013).
37. Feng, D. *et al.* Zirconium-Metalloporphyrin PCN-222: Mesoporous Metal–Organic Frameworks with Ultrahigh Stability as Biomimetic Catalysts. *Angew. Chem. Int. Ed.* **51**, 10307–10310 (2012).
38. Feng, D. *et al.* Kinetically tuned dimensional augmentation as a versatile synthetic route towards robust metal–organic frameworks. *Nat. Commun.* **5**, 5723 (2014).
39. Gaab, M., Trukhan, N., Maurer, S., Gummaraju, R. & Müller, U. The progression of Al-based metal-organic frameworks – From academic research to industrial production and applications. *Microporous Mesoporous Mater.* **157**, 131–136 (2012).
40. Farrusseng, D., Aguado, S. & Pinel, C. Metal-Organic Frameworks: Opportunities for Catalysis. *Angew. Chem. Int. Ed.* **48**, 7502–7513 (2009).
41. Allendorf, M. D., Bauer, C. A., Bhakta, R. K. & Houk, R. J. T. Luminescent metal–organic frameworks. *Chem. Soc. Rev.* **38**, 1330 (2009).
42. Stock, N. & Biswas, S. Synthesis of Metal-Organic Frameworks (MOFs): Routes to Various MOF Topologies, Morphologies, and Composites. *Chem. Rev.* **112**, 933–969 (2012).
43. Reinsch, H., Waitschat, S., Chavan, S. M., Lillerud, K. P. & Stock, N. A Facile ‘Green’ Route for Scalable Batch Production and Continuous Synthesis of Zirconium MOFs. *Eur. J. Inorg. Chem.* **2016**, 4490–4498 (2016).
44. Sun, Y. & Zhou, H.-C. Recent progress in the synthesis of metal–organic frameworks. *Sci. Technol. Adv. Mater.* **16**, 054202 (2015).
45. Mueller, U. *et al.* Method for Electrochemical Production of a Crystalline Porous Metal Organic Skeleton Material. (2006).
46. Chang, J. S., Jung, S. H. & Hwang, J. S. A Synthesis Method of Porous Organic-Inorganic Hybrid Materials. (2006).
47. James, S. L., Lazuen-Garay, A. & Pichon, A. Use of grinding in chemical synthesis. (2006).

48. Maspoch, C. D. *et al.* Method for the preparation of metal organic frameworks. (2016).
49. RUBIO, M. M. *et al.* Production of metal-organic frameworks. (2016).
50. Mueller, U. *et al.* Metal–organic frameworks—prospective industrial applications. *J Mater Chem* **16**, 626–636 (2006).
51. Taddei, M., Steitz, D. A., van Bokhoven, J. A. & Ranocchiari, M. Continuous-Flow Microwave Synthesis of Metal-Organic Frameworks: A Highly Efficient Method for Large-Scale Production. *Chem. - Eur. J.* **22**, 3245–3249 (2016).
52. Li, W.-J., Tu, M., Cao, R. & Fischer, R. A. Metal–organic framework thin films: electrochemical fabrication techniques and corresponding applications & perspectives. *J Mater Chem A* **4**, 12356–12369 (2016).
53. Al-Kutubi, H., Gascon, J., Sudhölter, E. J. R. & Rassaei, L. Electrosynthesis of Metal-Organic Frameworks: Challenges and Opportunities. *ChemElectroChem* **2**, 462–474 (2015).
54. Dincă, M. & Li, M. Methods for electrochemically induced cathodic deposition of crystalline metal-organic frameworks.
55. Campagnol, N. *et al.* On the electrochemical deposition of metal–organic frameworks. *J Mater Chem A* **4**, 3914–3925 (2016).
56. Schäfer, P., van der Veen, M. A. & Domke, K. F. Unraveling a two-step oxidation mechanism in electrochemical Cu-MOF synthesis. *Chem Commun* **52**, 4722–4725 (2016).
57. Ameloot, R. *et al.* Patterned Growth of Metal-Organic Framework Coatings by Electrochemical Synthesis. *Chem. Mater.* **21**, 2580–2582 (2009).
58. Martinez Joaristi, A., Juan-Alcañiz, J., Serra-Crespo, P., Kapteijn, F. & Gascon, J. Electrochemical Synthesis of Some Archetypical Zn<sup>2+</sup>, Cu<sup>2+</sup>, and Al<sup>3+</sup> Metal Organic Frameworks. *Cryst. Growth Des.* **12**, 3489–3498 (2012).
59. Van Assche, T. R. C. *et al.* Electrochemical synthesis of thin HKUST-1 layers on copper mesh. *Microporous Mesoporous Mater.* **158**, 209–213 (2012).

60. Gascon, J., Aguado, S. & Kapteijn, F. Manufacture of dense coatings of Cu<sub>3</sub>(BTC)<sub>2</sub> (HKUST-1) on  $\alpha$ -alumina. *Micro. Meso. Mat.* **113**, 132–138 (2008).
61. Van Assche, T. R. C. *et al.* On controlling the anodic electrochemical film deposition of HKUST-1 metal–organic frameworks. *Microporous Mesoporous Mater.* **224**, 302–310 (2016).
62. Van Assche, T. R. C. *et al.* Electrochemical synthesis of thin HKUST-1 layers on copper mesh. *Microporous Mesoporous Mater.* **158**, 209–213 (2012).
63. Hartmann, M. *et al.* Adsorptive Separation of Isobutene and Isobutane on Cu<sub>3</sub>(BTC)<sub>2</sub>. *Langmuir* **24**, 8634–8642 (2008).
64. Campagnol, N. *et al.* High pressure, high temperature electrochemical synthesis of metal–organic frameworks: films of MIL-100 (Fe) and HKUST-1 in different morphologies. *J. Mater. Chem. A* **1**, 5827 (2013).
65. Worrall, S. D. *et al.* Electrochemical deposition of zeolitic imidazolate framework electrode coatings for supercapacitor electrodes. *Electrochimica Acta* **197**, 228–240 (2016).
66. Campagnol, N., Souza, E. R., De Vos, D. E., Binnemans, K. & Fransaer, J. Luminescent terbium-containing metal–organic framework films: new approaches for the electrochemical synthesis and application as detectors for explosives. *Chem Commun* **50**, 12545–12547 (2014).
67. Li, W.-J., Lü, J., Gao, S.-Y., Li, Q.-H. & Cao, R. Electrochemical preparation of metal–organic framework films for fast detection of nitro explosives. *J Mater Chem A* **2**, 19473–19478 (2014).
68. Yang, H. M. *et al.* Electrochemical synthesis of flower shaped morphology MOFs in an ionic liquid system and their electrocatalytic application to the hydrogen evolution reaction. *RSC Adv* **4**, 15720–15726 (2014).
69. Yang, H. *et al.* In situ electrochemical synthesis of MOF-5 and its application in improving photocatalytic activity of BiOBr. *Trans. Nonferrous Met. Soc. China* **25**, 3987–3994 (2015).
70. Li, M. & Dincă, M. Reductive Electrosynthesis of Crystalline Metal–Organic Frameworks. *J. Am. Chem. Soc.* **133**, 12926–12929 (2011).

71. Li, M. & Dincă, M. On the Mechanism of MOF-5 Formation under Cathodic Bias. *Chem. Mater.* **27**, 3203–3206 (2015).
72. Li, M. & Dincă, M. Selective formation of biphasic thin films of metal–organic frameworks by potential-controlled cathodic electrodeposition. *Chem Sci* **5**, 107–111 (2014).
73. Zhu, H., Liu, H., Zhitomirsky, I. & Zhu, S. Preparation of metal–organic framework films by electrophoretic deposition method. *Mater. Lett.* **142**, 19–22 (2015).
74. Hod, I. *et al.* Directed Growth of Electroactive Metal-Organic Framework Thin Films Using Electrophoretic Deposition. *Adv. Mater.* **26**, 6295–6300 (2014).
75. Ameloot, R. *et al.* Patterned film growth of metal–organic frameworks based on galvanic displacement. *Chem. Commun.* **46**, 3735 (2010).
76. Stassen, I. *et al.* Electrochemical Film Deposition of the Zirconium Metal–Organic Framework UiO-66 and Application in a Miniaturized Sorbent Trap. *Chem. Mater.* **27**, 1801–1807 (2015).
77. Yadnum, S. *et al.* Site-Selective Synthesis of Janus-type Metal-Organic Framework Composites. *Angew. Chem.* **126**, 4082–4086 (2014).
78. Bilecka, I. & Niederberger, M. Microwave chemistry for inorganic nanomaterials synthesis. *Nanoscale* **2**, 1358–1374 (2010).
79. Gharibeh, M., Tompsett, G. A., Yngvesson, K. S. & Conner, W. C. Microwave synthesis of zeolites: effect of power delivery. *J. Phys. Chem. B* **113**, 8930–8940 (2009).
80. Khan, N. A. & Jung, S. H. Synthesis of metal-organic frameworks (MOFs) with microwave or ultrasound: Rapid reaction, phase-selectivity, and size reduction. *Coord. Chem. Rev.* **285**, 11–23 (2015).
81. Hoz, A. de la, Díaz-Ortiz, Á. & Moreno, A. Microwaves in organic synthesis. Thermal and non-thermal microwave effects. *Chem. Soc. Rev.* **34**, 164–178 (2005).
82. Jung, S.-H., Lee, J.-H. & Chang, J.-S. Microwave Synthesis of a Nanoporous Hybrid Material, Chromium Trimesate. *Bull. Korean Chem. Soc.* **26**, 880–881 (2005).

83. Jhung, S. H. *et al.* Microwave Synthesis of Chromium Terephthalate MIL-101 and Its Benzene Sorption Ability. *Adv. Mater.* **19**, 121–124 (2007).
84. Ni, Z. & Masel, R. I. Rapid Production of Metal–Organic Frameworks via Microwave-Assisted Solvothermal Synthesis. *J. Am. Chem. Soc.* **128**, 12394–12395 (2006).
85. Choi, J.-S., Son, W.-J., Kim, J. & Ahn, W.-S. Metal–organic framework MOF-5 prepared by microwave heating: Factors to be considered. *Microporous Mesoporous Mater.* **116**, 727–731 (2008).
86. Taylor-Pashow, K. M. L., Rocca, J. D., Xie, Z., Tran, S. & Lin, W. Postsynthetic Modifications of Iron-Carboxylate Nanoscale Metal–Organic Frameworks for Imaging and Drug Delivery. *J. Am. Chem. Soc.* **131**, 14261–14263 (2009).
87. Khan, N. A. & Jhung, S.-H. Facile Syntheses of Metal-organic Framework Cu(BTC)<sub>2</sub>(H<sub>2</sub>O)<sub>3</sub> under Ultrasound. *Bull. Korean Chem. Soc.* **30**, 2921–2926 (2009).
88. Jung, D.-W., Yang, D.-A., Kim, J., Kim, J. & Ahn, W.-S. Facile synthesis of MOF-177 by a sonochemical method using 1-methyl-2-pyrrolidinone as a solvent. *Dalton Trans.* **39**, 2883–2887 (2010).
89. Khan, N. A., Kang, I. J., Seok, H. Y. & Jhung, S. H. Facile synthesis of nano-sized metal-organic frameworks, chromium-benzenedicarboxylate, MIL-101. *Chem. Eng. J.* **166**, 1152–1157 (2011).
90. Haque, E. & Jhung, S. H. Synthesis of isostructural metal–organic frameworks, CPO-27s, with ultrasound, microwave, and conventional heating: Effect of synthesis methods and metal ions. *Chem. Eng. J.* **173**, 866–872 (2011).
91. Haque, E., Khan, N. A., Park, J. H. & Jhung, S. H. Synthesis of a Metal–Organic Framework Material, Iron Terephthalate, by Ultrasound, Microwave, and Conventional Electric Heating: A Kinetic Study. *Chem. – Eur. J.* **16**, 1046–1052 (2010).
92. Chalati, T., Horcajada, P., Gref, R., Couvreur, P. & Serre, C. Optimisation of the synthesis of MOF nanoparticles made of flexible porous iron fumarate MIL-88A. *J. Mater. Chem.* **21**, 2220–2227 (2011).

93. Park, J.-H., Park, S.-H. & Jhung, S.-H. Microwave-Syntheses of Zeolitic Imidazolate Framework Material, ZIF-8. *J. Korean Chem. Soc.* **53**, 553–559 (2009).
94. Silva, P., Valente, A. A., Rocha, J. & Almeida Paz, F. A. Fast Microwave Synthesis of a Microporous Lanthanide–Organic Framework. *Cryst. Growth Des.* **10**, 2025–2028 (2010).
95. Vilela, S. M. F. *et al.* Multifunctional micro- and nanosized metal–organic frameworks assembled from bisphosphonates and lanthanides. *J. Mater. Chem. C* **2**, 3311–3327 (2014).
96. Bag, P. P., Wang, X.-S. & Cao, R. Microwave-assisted large scale synthesis of lanthanide metal–organic frameworks (Ln-MOFs), having a preferred conformation and photoluminescence properties. *Dalton Trans.* **44**, 11954–11962 (2015).
97. Liang, W. & D’Alessandro, D. M. Microwave-assisted solvothermal synthesis of zirconium oxide based metal–organic frameworks. *Chem. Commun.* **49**, 3706–3708 (2013).
98. Taddei, M. *et al.* Efficient microwave assisted synthesis of metal–organic framework UiO-66: optimization and scale up. *Dalton Trans.* **44**, 14019–14026 (2015).
99. Liang, W. *et al.* Defect engineering of UiO-66 for CO<sub>2</sub> and H<sub>2</sub>O uptake – a combined experimental and simulation study. *Dalton Trans.* **45**, 4496–4500 (2016).
100. Garay, A. L., Pichon, A. & James, S. L. Solvent-free synthesis of metal complexes. *Chem. Soc. Rev.* **36**, 846–855 (2007).
101. Kaupp, G. Solid-state molecular syntheses: complete reactions without auxiliaries based on the new solid-state mechanism. *CrystEngComm* **5**, 117–133 (2003).
102. Friščić, T. Supramolecular concepts and new techniques in mechanochemistry: cocrystals, cages, rotaxanes, open metal–organic frameworks. *Chem. Soc. Rev.* **41**, 3493–3510 (2012).
103. *Mechanochemistry in Nanoscience and Minerals Engineering | Peter Balaz | Springer.*
104. Boldyrev, V. V. Mechanochemistry and mechanical activation of solids. *Solid State Ion.* **63**, 537–543 (1993).
105. Stolle, A., Szuppa, T., Leonhardt, S. E. S. & Ondruschka, B. Ball milling in organic synthesis: solutions and challenges. *Chem. Soc. Rev.* **40**, 2317–2329 (2011).



106. Crawford, D. E. & Casaban, J. Recent Developments in Mechanochemical Materials Synthesis by Extrusion. *Adv. Mater.* **28**, 5747–5754 (2016).
107. L. James, S. *et al.* Mechanochemistry: opportunities for new and cleaner synthesis. *Chem. Soc. Rev.* **41**, 413–447 (2012).
108. Braga, D. & Grepioni, F. Making crystals from crystals: a green route to crystal engineering and polymorphism. *Chem. Commun.* 3635–3645 (2005). doi:10.1039/B504668H
109. Friščić, T. New opportunities for materials synthesis using mechanochemistry. *J. Mater. Chem.* **20**, 7599–7605 (2010).
110. Pichon, A., Lazuen-Garay, A. & James, S. L. Solvent-free synthesis of a microporous metal–organic framework. *CrystEngComm* **8**, 211–214 (2006).
111. Pichon, A. & L. James, S. An array-based study of reactivity under solvent -free mechanochemical conditions—insights and trends. *CrystEngComm* **10**, 1839–1847 (2008).
112. Tanaka, S., Kida, K., Nagaoka, T., Ota, T. & Miyake, Y. Mechanochemical dry conversion of zinc oxide to zeolitic imidazolate framework. *Chem. Commun.* **49**, 7884–7886 (2013).
113. Singh, N. K., Hardi, M. & Balema, V. P. Mechanochemical synthesis of an yttrium based metal–organic framework. *Chem. Commun.* **49**, 972–974 (2013).
114. Leng, K., Sun, Y., Li, X., Sun, S. & Xu, W. Rapid Synthesis of Metal–Organic Frameworks MIL-101(Cr) Without the Addition of Solvent and Hydrofluoric Acid. *Cryst. Growth Des.* **16**, 1168–1171 (2016).
115. Braga, D. *et al.* Simple and Quantitative Mechanochemical Preparation of a Porous Crystalline Material Based on a 1D Coordination Network for Uptake of Small Molecules. *Angew. Chem. Int. Ed.* **45**, 142–146 (2006).
116. Friščić, T. & Fábián, L. Mechanochemical conversion of a metal oxide into coordination polymers and porous frameworks using liquid-assisted grinding (LAG). *CrystEngComm* **11**, 743–745 (2009).

117. Klimakow, M., Klobes, P., Thünemann, A. F., Rademann, K. & Emmerling, F. Mechanochemical Synthesis of Metal–Organic Frameworks: A Fast and Facile Approach toward Quantitative Yields and High Specific Surface Areas. *Chem. Mater.* **22**, 5216–5221 (2010).
118. Yuan, W. *et al.* Study of the mechanochemical formation and resulting properties of an archetypal MOF: Cu<sub>3</sub>(BTC)<sub>2</sub> (BTC = 1,3,5-benzenetricarboxylate). *CrystEngComm* **12**, 4063–4065 (2010).
119. Fujii, K. *et al.* Direct structure elucidation by powder X-ray diffraction of a metal–organic framework material prepared by solvent-free grinding. *Chem. Commun.* **46**, 7572–7574 (2010).
120. Prochowicz, D. *et al.* A mechanochemical strategy for IRMOF assembly based on pre-designed oxo-zinc precursors. *Chem. Commun.* **51**, 4032–4035 (2015).
121. Užarević, K. *et al.* Mechanochemical and solvent-free assembly of zirconium-based metal–organic frameworks. *Chem. Commun.* **52**, 2133–2136 (2016).
122. Friščić, T. *et al.* Ion- and Liquid-Assisted Grinding: Improved Mechanochemical Synthesis of Metal–Organic Frameworks Reveals Salt Inclusion and Anion Templating. *Angew. Chem. Int. Ed.* **49**, 712–715 (2010).
123. Beldon, P. J. *et al.* Rapid Room-Temperature Synthesis of Zeolitic Imidazolate Frameworks by Using Mechanochemistry. *Angew. Chem. Int. Ed.* **49**, 9640–9643 (2010).
124. Samuel R. Percy. Improvement in drying and concentrating liquid substances by atomizing. (1872).
125. Patel, R. P., Patel, M. P. & Suthar, A. M. Spray drying technology: an overview. *Indian J. Sci. Technol.* **2**, 44–47 (2009).
126. Dimitris Charalampopoulos & Robert A. Rastall. *Prebiotics and Probiotics Science and Technology*. (Springer).
127. Okuyama, K., Abdullah, M., Wuled Lenggoro, I. & Iskandar, F. Preparation of functional nanostructured particles by spray drying. *Adv. Powder Technol.* **17**, 587–611 (2006).

128. Thiele, J. *et al.* Early development drug formulation on a chip: Fabrication of nanoparticles using a microfluidic spray dryer. *Lab. Chip* **11**, 2362 (2011).
129. Rivas-Murias, B. *et al.* Spray drying: An alternative synthesis method for polycationic oxide compounds. *J. Phys. Chem. Solids* **72**, 158–163 (2011).
130. Sun, R., Lu, Y. & Chen, K. Preparation and characterization of hollow hydroxyapatite microspheres by spray drying method. *Mater. Sci. Eng. C* **29**, 1088–1092 (2009).
131. Okuyama, K., Abdullah, M., Wuled Lenggoro, I. & Iskandar, F. Preparation of functional nanostructured particles by spray drying. *Adv. Powder Technol.* **17**, 587–611 (2006).
132. Carné-Sánchez, A., Imaz, I., Cano-Sarabia, M. & MasPOCH, D. A spray-drying strategy for synthesis of nanoscale metal–organic frameworks and their assembly into hollow superstructures. *Nat. Chem.* **5**, 203–211 (2013).
133. Garcia Marquez, A. *et al.* Green scalable aerosol synthesis of porous metal–organic frameworks. *Chem. Commun.* **49**, 3848 (2013).
134. Garzón-Tovar, L. *et al.* A spray-drying continuous-flow method for simultaneous synthesis and shaping of microspherical high nuclearity MOF beads. *React Chem Eng* **1**, 533–539 (2016).
135. Garzón-Tovar, L., Rodríguez-Hermida, S., Imaz, I. & MasPOCH, D. Spray Drying for Making Covalent Chemistry: Postsynthetic Modification of Metal–Organic Frameworks. *J. Am. Chem. Soc.* **139**, 897–903 (2017).
136. Guillerm, V. *et al.* Continuous One-Step Synthesis of Porous M-XF<sub>6</sub>-based Metal-Organic and Hydrogen-Bonded Frameworks. *Chem. – Eur. J.* n/a-n/a (2017). doi:10.1002/chem.201605507
137. Wang, Z. *et al.* Lanthanide-Organic Framework Nanothermometers Prepared by Spray-Drying. *Adv. Funct. Mater.* **25**, 2824–2830 (2015).
138. Carné-Sánchez, A. *et al.* Protecting Metal-Organic Framework Crystals from Hydrolytic Degradation by Spray-Dry Encapsulating Them into Polystyrene Microspheres. *Adv. Mater.* **27**, 869–873 (2015).

139. Garzón-Tovar, L., Pérez-Carvajal, J., Imaz, I. & Maspoch, D. Composite Salt in Porous Metal-Organic Frameworks for Adsorption Heat Transformation. *Adv. Funct. Mater.* **Submitted**,
140. Ameloot, R. *et al.* Interfacial synthesis of hollow metal–organic framework capsules demonstrating selective permeability. *Nat. Chem.* **3**, 382–387 (2011).
141. Faustini, M. *et al.* Microfluidic Approach toward Continuous and Ultra-Fast Synthesis of Metal-Organic Framework Crystals and Hetero-Structures in Confined Microdroplets. *J. Am. Chem. Soc.* 14619–14626 (2013). doi:10.1021/ja4039642
142. D'Arras, L. *et al.* Fast and Continuous Processing of a new sub- micronic Lanthanide-based Metal-Organic Framework. *New J. Chem.* (2014). doi:10.1039/c3nj01371e
143. Polyzoidis, A., Altenburg, T., Schwarzer, M., Loebbecke, S. & Kaskel, S. Continuous microreactor synthesis of ZIF-8 with high space–time-yield and tunable particle size. *Chem. Eng. J.* **283**, 971–977 (2016).
144. Tai, S. *et al.* Facile preparation of UiO-66 nanoparticles with tunable sizes in a continuous flow microreactor and its application in drug delivery. *Microporous Mesoporous Mater.* **220**, 148–154 (2016).
145. Gimeno-Fabra, M. *et al.* Instant MOFs: continuous synthesis of metal–organic frameworks by rapid solvent mixing. *Chem. Commun.* **48**, 10642–10644 (2012).
146. Munn, A. S., Dunne, P. W., Tang, S. V. Y. & Lester, E. H. Large-scale continuous hydrothermal production and activation of ZIF-8. *Chem Commun* (2015). doi:10.1039/C5CC04636J
147. Bayliss, P. A. *et al.* Synthesis of metal–organic frameworks by continuous flow. *Green Chem.* **16**, 3796 (2014).
148. Kim, K.-J. *et al.* High-rate synthesis of Cu–BTC metal–organic frameworks. *Chem. Commun.* **49**, 11518 (2013).
149. Rubio-Martinez, M. *et al.* Versatile, High Quality and Scalable Continuous Flow Production of Metal-Organic Frameworks. *Sci. Rep.* **4**, (2014).

150. Rubio-Martinez, M. *et al.* Scalability of Continuous Flow Production of Metal–Organic Frameworks. *ChemSusChem* **9**, 938–941 (2016).
151. Waitschat, S., Wharmby, M. T. & Stock, N. Flow-synthesis of carboxylate and phosphonate based metal–organic frameworks under non-solvothermal reaction conditions. *Dalton Trans.* **44**, 11235–11240 (2015).
152. Albuquerque, G. H. *et al.* Gas–liquid segmented flow microwave-assisted synthesis of MOF-74(Ni) under moderate pressures. *CrystEngComm* **17**, 5502–5510 (2015).
153. Taddei, M., Steitz, D. A., van Bokhoven, J. A. & Ranocchiari, M. Continuous-Flow Microwave Synthesis of Metal–Organic Frameworks: A Highly Efficient Method for Large-Scale Production. *Chem. – Eur. J.* **22**, 3245–3249 (2016).
154. Schoenecker, P. M., Belancik, G. A., Grabicka, B. E. & Walton, K. S. Kinetics study and crystallization process design for scale-up of UiO-66-NH<sub>2</sub> synthesis. *AIChE J.* **59**, 1255–1262 (2013).
155. McKinsty, C. *et al.* Scalable continuous solvothermal synthesis of metal organic framework (MOF-5) crystals. *Chem. Eng. J.* **285**, 718–725 (2016).
156. Ulrich, G. D. *Chemical engineering process design and economics: a practical guide.* (Process Pub, 2004).
157. E. Mondloch, J., Karagiari, O., K. Farha, O. & T. Hupp, J. Activation of metal–organic framework materials. *CrystEngComm* **15**, 9258–9264 (2013).
158. Wang, L. J. *et al.* Synthesis and Characterization of Metal–Organic Framework-74 Containing 2, 4, 6, 8, and 10 Different Metals. *Inorg. Chem.* **53**, 5881–5883 (2014).
159. Park, K. S. *et al.* Exceptional chemical and thermal stability of zeolitic imidazolate frameworks. *Proc. Natl. Acad. Sci.* **103**, 10186–10191 (2006).
160. An, J. *et al.* Metal-adeninate vertices for the construction of an exceptionally porous metal–organic framework. *Nat. Commun.* **3**, 604 (2012).

161. Koh, K., Oosterhout, J. D. V., Roy, S., Wong-Foy, A. G. & Matzger, A. J. Exceptional surface area from coordination copolymers derived from two linear linkers of differing lengths. *Chem. Sci.* **3**, 2429–2432 (2012).
162. He, Y.-P., Tan, Y.-X. & Zhang, J. Comparative Study of Activation Methods on Tuning Gas Sorption Properties of a Metal–Organic Framework with Nanosized Ligands. *Inorg. Chem.* **51**, 11232–11234 (2012).
163. Rubio-Martinez, M. *et al.* Scalable simultaneous activation and separation of metal–organic frameworks. *RSC Adv.* **6**, 5523–5527 (2016).
164. Yu, M. *et al.* Covalent immobilization of metal–organic frameworks onto the surface of nylon—a new approach to the functionalization and coloration of textiles. *Sci. Rep.* **6**, 22796 (2016).
165. Garai, B., Mallick, A. & Banerjee, R. Photochromic metal–organic frameworks for inkless and erasable printing. *Chem Sci* **7**, 2195–2200 (2016).
166. Wu, Y. *et al.* Electrospun fibrous mats as skeletons to produce free-standing MOF membranes. *J. Mater. Chem.* **22**, 16971 (2012).
167. Qiu, S., Xue, M. & Zhu, G. Metal–organic framework membranes: from synthesis to separation application. *Chem Soc Rev* **43**, 6116–6140 (2014).
168. Zhang, Y. *et al.* Constructing Free Standing Metal Organic Framework MIL-53 Membrane Based on Anodized Aluminum Oxide Precursor. *Sci. Rep.* **4**, (2014).
169. Ren, J., Langmi, H. W., North, B. C. & Mathe, M. Review on processing of metal-organic framework (MOF) materials towards system integration for hydrogen storage: Review on processing of MOF materials towards system integration. *Int. J. Energy Res.* **39**, 607–620 (2015).
170. Wang, Z. *et al.* Monolithic, Crystalline MOF Coating: An Excellent Patterning and Photoresist Material. *ChemNanoMat* **1**, 338–345 (2015).
171. Beckner, M. & Dailly, A. Adsorbed methane storage for vehicular applications. *Appl. Energy* **149**, 69–74 (2015).

172. Hesse, M., Müller, U. & Yaghi, O. M. Shaped bodies containing metal-organic frameworks.
173. Kim, J., Kim, S.-H., Yang, S.-T. & Ahn, W.-S. Bench-scale preparation of Cu<sub>3</sub>(BTC)<sub>2</sub> by ethanol reflux: Synthesis optimization and adsorption/catalytic applications. *Microporous Mesoporous Mater.* **161**, 48–55 (2012).
174. Bazer-Bachi, D., Assié, L., Lecocq, V., Harbuzaru, B. & Falk, V. Towards industrial use of metal-organic framework: Impact of shaping on the MOF properties. *Powder Technol.* **255**, 52–59 (2014).
175. Peterson, G. W. *et al.* Effects of pelletization pressure on the physical and chemical properties of the metal–organic frameworks Cu<sub>3</sub>(BTC)<sub>2</sub> and UiO-66. *Microporous Mesoporous Mater.* **179**, 48–53 (2013).
176. Tagliabue, M. *et al.* Methane storage on CPO-27-Ni pellets. *J. Porous Mater.* **18**, 289–296 (2011).
177. Chapman, K. W., Halder, G. J. & Chupas, P. J. Pressure-Induced Amorphization and Porosity Modification in a Metal–Organic Framework. *J. Am. Chem. Soc.* **131**, 17546–17547 (2009).
178. Cavenati, S., Grande, C. A., Rodrigues, A. E., Kiener, C. & Müller, U. Metal Organic Framework Adsorbent for Biogas Upgrading. *Ind. Eng. Chem. Res.* **47**, 6333–6335 (2008).
179. Finsy, V. *et al.* Separation of CO<sub>2</sub>/CH<sub>4</sub> mixtures with the MIL-53(Al) metal–organic framework. *Microporous Mesoporous Mater.* **120**, 221–227 (2009).
180. Küsgens, P., Zgaverdea, A., Fritz, H.-G., Siegle, S. & Kaskel, S. Metal-Organic Frameworks in Monolithic Structures: Rapid Communications of the American Ceramic Society. *J. Am. Ceram. Soc.* **93**, 2476–2479 (2010).
181. Ren, J. *et al.* A more efficient way to shape metal-organic framework (MOF) powder materials for hydrogen storage applications. *Int. J. Hydrog. Energy* **40**, 4617–4622 (2015).
182. Ren, J., Segakweng, T., Langmi, H. W., North, B. C. & Mathe, M. Ni foam-immobilized MIL-101(Cr) nanocrystals toward system integration for hydrogen storage. *J. Alloys Compd.* **645**, S170–S173 (2015).

183. Betke, U. *et al.* Micro-Macroporous Composite Materials: SiC Ceramic Foams Functionalized With the Metal Organic Framework HKUST-1. *Chem. Ing. Tech.* **88**, 264–273 (2016).
184. Pinto, M. L., Dias, S. & Pires, J. Composite MOF Foams: The Example of UiO-66/Polyurethane. *ACS Appl. Mater. Interfaces* **5**, 2360–2363 (2013).
185. Chen, Y. *et al.* Shaping of Metal–Organic Frameworks: From Fluid to Shaped Bodies and Robust Foams. *J. Am. Chem. Soc.* **138**, 10810–10813 (2016).
186. Zhao, J. *et al.* Highly Adsorptive, MOF-Functionalized Nonwoven Fiber Mats for Hazardous Gas Capture Enabled by Atomic Layer Deposition. *Adv. Mater. Interfaces* **1**, 1400040 (2014).
187. Spjelkavik, A. I., Aarti, Divekar, S., Didriksen, T. & Blom, R. Forming MOFs into Spheres by Use of Molecular Gastronomy Methods. *Chem. – Eur. J.* **20**, 8973–8978 (2014).
188. Aguado, S., Canivet, J. & Farrusseng, D. Facile shaping of an imidazolate-based MOF on ceramic beads for adsorption and catalytic applications. *Chem. Commun.* **46**, 7999 (2010).
189. MOF Technologies Announces World’s First Commercial Application of Metal Organic Framework Technology by Decco Worldwide at MOF 2016. *MOF Technologies* (2016).
190. 2016, R. T. O. MOFs offer safer toxic gas storage. *Chemistry World* Available at: <https://www.chemistryworld.com/news/mofs-offer-safer-toxic-gas-storage-/1017610.article>. (Accessed: 8th February 2017)
191. Fundamentals and Applications of Advanced Porous Materials - CSIRO. *Fundamentals and Applications of Advanced Porous Materials - CSIRO* Available at: <https://events.csiro.au/Events/2016/June/23/Advanced-Porous-Materials>. (Accessed: 8th February 2017)
192. Frameworks for commercial success. *Nat. Chem.* **8**, 987–987 (2016).
193. MOFapps - News. <http://mofapps.com/news.html> Available at: <http://mofapps.com/news.html>. (Accessed: 8th February 2017)
194. ProDIA. Available at: <http://prodia-mof.eu/>. (Accessed: 27th March 2017)



195. Dreischarf, A. C., Lammert, M., Stock, N. & Reinsch, H. Green Synthesis of Zr-CAU-28: Structure and Properties of the First Zr-MOF Based on 2,5-Furandicarboxylic Acid. *Inorg. Chem.* (2017). doi:10.1021/acs.inorgchem.6b02969
196. Waitschat, S., Reinsch, H. & Stock, N. Water-based synthesis and characterisation of a new Zr-MOF with a unique inorganic building unit. *Chem. Commun.* **52**, 12698–12701 (2016).
197. Discover our MOF products | ProfMOF. <http://profmof.com/discover-our-mof-products/> Available at: <http://profmof.com/discover-our-mof-products/>. (Accessed: 8th February 2017)
198. MOF. <https://secure.strem.com/catalog/family/MOF/> Available at: <https://secure.strem.com/catalog/family/MOF/>. (Accessed: 8th February 2017)
199. Metal Organic Frameworks. <http://www.sigmaaldrich.com/technical-documents/articles/materials-science/metal-organic-frameworks.html> Available at: <http://www.sigmaaldrich.com/technical-documents/articles/materials-science/metal-organic-frameworks.html>. (Accessed: 8th February 2017)
200. Home. <https://www.mofworx.com/> Available at: <https://www.mofworx.com/>. (Accessed: 8th February 2017)
201. theMOFcompany. <http://themofcompany.com>
202. framergy. <http://www.framergy.com/> Available at: <http://www.framergy.com/>. (Accessed: 8th February 2017)
203. ACSYNAM. <https://acsynam.com/> Available at: <https://acsynam.com/>. (Accessed: 8th February 2017)
204. Promethean to Showcase Manufacturing Capability with MOF production. <http://www.prometheanparticles.co.uk/promethean-to-showcase-manufacturing-capability-with-mof-production/> (2016). Available at: <http://www.prometheanparticles.co.uk/promethean-to-showcase-manufacturing-capability-with-mof-production/>. (Accessed: 8th February 2017)
205. Mueller, U. *et al.* Organometallic Framework Material, Preparation and Use. (2006).

206. James, S., Lazuen-Garay, A. & Pichon, A. Chemical Synthesis. (2007).
207. Koch, M. & Jonschker, G. Monolithic Materials for Gas Stores. (2010).
208. Allendorf, M. D. & Hesketh, P. J. Method and apparatus for detecting an analyte. (2011).
209. Lee, U.-H. *et al.* Method for Preparing Porous Organic-Inorganic Hybrid Materials. (2014).
210. Schroder, M., Poliakoff, M., Bayliss, P. & Velilla, E. Metal-Organic Frameworks. (2014).
211. Unpublished work.
212. Moreira, M. A. *et al.* Reverse Shape Selectivity in the Liquid-Phase Adsorption of Xylene Isomers in Zirconium Terephthalate MOF UiO-66. *Langmuir* **28**, 5715–5723 (2012).